Exploring the Role of Natural Antisense Transcripts in the Stress Response of *Ustilago maydis*

A thesis submitted to the Committee of Graduate Studies

in partial fulfillment of the requirements for the degree of

Master of Science

in the faculty of Arts and Science

TRENT UNIVERSITY

Peterborough, Ontario, Canada

Environmental and Life Sciences M.Sc. Graduate Program

January 2023

ABSTRACT

Exploring the role of natural antisense transcripts in the stress response of *Ustilago maydis*

Monique Lariviere

Fungal pathogens adapt to environmental changes faster than their hosts, due in part to their adaptive mechanisms exhibited in response to stress. *Ustilago maydis* was used to investigate potential natural antisense transcript (NAT) RNA-mediated mechanisms that enhance fungal adaptation to stress. Of the 349 NATs conserved amongst *U. maydis* and two related smut fungi, five NATs were identified as having altered transcript levels in response to multiple stress conditions. Subsequently, antisense transcript expression vectors were created for select NATs and transformed into *U. maydis* haploid cells. When exposed to stress conditions, two antisense expressing mutant strains exhibited alterations in growth. RT-qPCR analysis of mRNA complementary to expressed NATs revealed no significant change in mRNA levels, which suggests NAT expression may influence stress response through dsRNA formation or other RNA mediated mechanisms. These results establish a basis for further investigations into the connection between NATs and the stress response of fungi.

KEYWORDS: *Ustilago maydis,* natural antisense transcripts, non-coding RNAs, stress response

ACKNOWLEDGEMENTS

I would like to thank my supervisor, Dr. Barry Saville for encouraging me to take the leap and pursue my M.Sc. degree. Thank you for listening to my ideas and helping me form a project around them, without your knowledge and support this research would not have been possible. I would also like to thank my committee members, Dr. Michael Donaldson, and Dr. Craig Brunetti, for providing insight and offering suggestions and support throughout my degree. Additionally, I would like to thank individuals at the School of Graduate Studies and the Environmental and Life Sciences Graduate Program office for their administrative support. I am also very grateful for the financial support from Trent University, Ontario Graduate Scholarship, and NSERC CGS-M.

To the past and present members of the Saville Lab, thank you for all your support and encouragement throughout all the ups and downs of the past couple of years. Without the guidance and training provided by the individuals in this lab, I would not be where I am today. Thank you, Amanda Seto and Emma Kaszecki, for always being there to listen and offer suggestions when research was not going well and also being ready to celebrate with me when it did. A special thank you to Victoria Kennedy for taking the time to train me, for talking me through my ideas when I thought I was going crazy, sitting on the floor of the lab with me when things started to go sideways, and always being willing to take coffee breaks. Most of all I would like to thank Emilee Storfie for being my constant sounding board for both science and life. These past couple of years have been a roller-coaster and I cannot imagine making it through this degree without your support. The endless phone calls and the times spent drinking over facetime celebrating our wins, deliberating over millions of potential outcomes, and talking each other out of worse case scenarios have been some

of the most memorable moments I have experienced during my time at Trent. Thank you for being there throughout it all and helping to guide me through the chaos that is graduate school.

Finally, I would like to thank my friends and family both near and far. Thank you for supporting me throughout my crazy hours and the chaos my life has been for the past couple of years. Thank you for always being willing to listen to my struggles with science and provide the comedic relief I needed when the stress started to get the better of me.

Table of Contents

ABSTRACT ..... *ii*

ACKNOWLEDGEMENTS ..... *iii*

LIST OF FIGURES ..... *viii*

LIST OF TABLES ..... *x*

LIST OF ABBREVIATIONS ..... *xi*

CHAPTER ONE: GENERAL INTRODUCTION *1*

CHAPTER TWO: LITERATURE REVIEW *5*

2.1 Fungal plant pathogens **5**

2.2 Biotrophic plant – pathogen interactions **6**

2.3 Fungal stress responses **9**

2.4 *Ustilago maydis* **12**

2.5 Natural antisense transcripts (NATs) **15**

2.6 Research objectives **18**

CHAPTER THREE: MATERIALS & METHODS *19*

3.1 Strains and growth conditions **19**

3.2 Liquid growth and plate assays **21**

3.3 Microscopy **23**

3.4 Primer and probe design **23**

3.5 Total RNA isolation, DNaseI treatment, reverse transcription, and transcript level analysis 28

3.6 Identification of NATs of interest 29

3.7 Creation of antisense expression constructs 30

3.8 Preparation of competent protoplasts and *U. maydis* transformation 34

CHAPTER FOUR: RESULTS 36

4.1 Assessing the impact of stress on the growth rate of *U. maydis* haploid strain 521 36

4.2 Selection of NATs 39

4.3 Assessment of NAT expression in response to single stressors 41

4.4 Assessment of NAT expression in response to staggered stressors 46

4.5 Impact of NAT expression on phenotype 48

4.5.1 521[pCMas-UMAG_00282*]* 49

4.5.2 521[pCMas-UMAG_01504*]* 51

4.5.3 521[pCMas-UMAG_05213*]* 52

4.5.4 521[pCMas-UMAG_10421*]* 54

4.6 Determining impact of NAT expression on complementary mRNA 55

4.6.1 521[pCMas-UMAG_01504*]* 56

4.6.2 521[pCMas-UMAG_10421*]* 59

CHAPTER FIVE: DISCUSSION 62

5.1 Assessing the impact of stress on the growth rate of *U. maydis* haploid strain 521 63

5.2 Identification and analysis of NATs with altered expression levels in response to stressed conditions 66

5.2.1 as-UMAG_00282 67

5.2.2 as-UMAG_01504 69

5.2.3 as-UMAG_05213 70

5.2.4 as-UMAG_06063 71

5.2.5 as-UMAG_10421 73

5.3 Future directions 76

CHAPTER SIX: CONCLUSION 78

REFERENCES 80

LIST OF FIGURES

Figure 1. *Ustilago maydis* life cycle inside Zea mays. 14

Figure 2. The growth rates of 521 haploid cells grown under oxidative conditions of 1.0 and 2.0 mM H_2O_2 are reduced compared to a 0.0 mM H_2O_2 control. 37

Figure 3. *U. maydis* haploid strain 521 exhibits altered growth in response to single stressors. 38

Figure 4. *U. maydis* haploid strain 521 exhibits altered growth in response to staggered stressors. 39

Figure 5. RT-PCR screen identified five NATs with altered transcript levels in multiple stressed conditions compared to the minimal media (MM) control. 44

Figure 6. RT-qPCR of NATs supported altered expression in stressed conditions compared to the minimal media (MM) control. 45

Figure 7. RT-qPCR of NATs indicates altered expression in staggered stressed conditions compared to the minimal media (MM) control. 48

Figure 8. Expression of NATs did not impact the morphology of haploid *U. maydis* cells. 49

Figure 9. 521[pCMas-*UMAG_00282*] does not exhibit altered growth in response to single stressors. 50

Figure 10. 521[pCMas-*UMAG_01504*] exhibits reduced growth in response to MM and MN conditions and increased growth in response to OX conditions 52

Figure 11. 521[pCMas-*UMAG_05213*] does not exhibit altered growth in response to single stressors. 53

Figure 12. 521[pCMas-*UMAG_10421*] exhibits reduced growth in MM conditions and increased growth in OX conditions. 55

Figure 13. Transformation of pCMas-*UMAG_01504* expression vector into *U. maydis* haploid cells increased NAT levels but did not impact the expression levels of the complementary mRNA. 58

Figure 14. Transformation of pCMas-*UMAG_10421* expression vector into *U. maydis* haploid cells increased NAT levels but did not impact the expression levels of the complementary mRNA. 60

LIST OF TABLES

Table 1. Strains used in this study.....21

Table 2. Primers used in this study 24

Table 3. Restriction enzymes used to create expression constructs.....34

Table 4. NATs complementary to genes with predicted links to stress response 40

Table 5. Summary of the nine NATs with altered expression in RT-PCR screen.....43

LIST OF ABBREVIATIONS

°C	degrees Celsius
3'	three-prime
5'	five-prime
Amp	Ampicillin
AP-1	activator protein 1
as	antisense
bp	base pair (s)
cDNA	complementary deoxyribonucleic acid
CO_2	carbon dioxide
CSR	core stress response
DEPC	diethylpyrocarbonate
dH_2O	deionized water
DNA	deoxyribonucleic acid
dsRNA	double-stranded ribonucleic acid
dT	oligo (dT)16
EST	expressed sequence tag
ETI	effector-triggered immunity
GAPDH	glyceraldehyde 3-phosphate dehydrogenase
gDNA	genomic deoxyribonucleic acid
H_2O	water
Hyg	hygromycin B resistance
HOG	high osmolarity glycerol
hrs	hours
ip	iron-sulphur protein
LB	Luria broth
lncRNA	long non-coding ribonucleic acid
M	marker
M	molar
MAPK	mitogen activated protein kinase
MC	minus carbon
mins	minutes
mL	millilitre (s)
mL^{-1}	per millilitre
mM	millimolar
MM	minimal medium
MN	minus nitrogen
mRNA	messenger ribonucleic acid
NAT	natural antisense transcript
ncRNA	non-coding ribonucleic acid
ng	nanogram (s)
NTC	no template control
OD_{600}	optical density
OS	osmotic
OX	oxidative

p	p-value (probability)
PAMP	pathogen associated molecular patterns
PCR	polymerase chain reaction
PDB	potato dextrose broth
PTI	PAMP-triggered immunity
RNA	ribonucleic acid
RNAi	RNA interference
RNA-seq	ribonucleic acid sequencing
ROS	reactive oxygen species
rpm	revolutions per minute
RT-PCR	reverse-transcriptase polymerase chain reaction
RT-qPCR	reverse-transcriptase quantitative polymerase chain reaction
s	second (s)
TAE	tris-acetate-ethylenediaminetetraacetic acid
U	unit (s)
v/v	volume by volume
W	water
w/v	weight by volume
YEPS	yeast extract peptone sucrose
µg	microgram (s)
µL	microliter (s)
μL^{-1}	per microliter

CHAPTER ONE: GENERAL INTRODUCTION

In 2018, the United Nations released their annual report on the Sustainable Development Goals, which included eradicating global hunger by 2030 (United Nations, 2018). Unfortunately, the combination of a global pandemic, growing conflict, and climate change have derailed this goal. Instead of reducing global hunger, it has continued to rise, with as many as 828 million people suffering in 2021 (United Nations, 2022a). The global pandemic and the conflict between Russia and Ukraine have exacerbated the rate of global hunger; however, climate change has been the leading cause of food insecurity since its initial rise in 2014 (Molotoks et al., 2021; United Nations, 2022a). Alterations in temperature, rainfall, evaporation patterns, and other extreme climactic conditions have caused adverse effects on the morphology, development, and molecular mechanisms of plants which ultimately cause a reduction in total crop yield (Chaudhry & Sidhu, 2022). The increase in global hunger, combined with a growing population predicted to reach 9.7 billion people by 2050, has emphasized the need to understand how climate variability will continue to impact global food crops (Molotoks et al., 2021; United Nations, 2022b).

As global population continues to rise, a 70-100% increase in crop production is required to mitigate the growing hunger crisis (Hussain et al., 2021; Tian et al., 2021). Typically, this increase in crop yield would require the expansion of cultivated land; however, the degree of expansion required to sustain these growing needs would lead to large-scale deforestation (Maja & Ayano, 2021). As the agricultural community is already acutely susceptible to the impacts of climate change, actions that would further exacerbate these impacts are not viable (Maja & Ayano, 2021; Molotoks et al., 2021). Instead, an emphasis has been placed on improving crop yields. Unfortunately, as efforts are made to

increase these yields, changes in temperature due to climate change have caused an estimated 3.1-7.4% loss in yield of major food crops per degree-Celsius increase in the global average temperature (Anderson et al., 2020; Molotoks et al., 2021). As climate change progresses, the increased prevalence of abiotic stressors will continue to impact plant growth negatively and, without sufficient management, could lead to a 70% reduction in total crop yield (Zulfiqar et al., 2019; Zulfiqar & Ashraf, 2021). Although these abiotic stressors pose a significant threat to global food security, the impact these changing conditions have on biotic stressors, including plant pathogens, must also be considered.

As the agricultural community continues to expand their research into technology focused on mitigating the direct impacts of climate change, an additional 10% of global food crops are lost due to diseases caused by plant pathogens (Bonghan Berinyuy et al., 2019; Donoso & Valenzuela, 2018). Although some aspects of climate change, including elevated CO_2 concentrations, can initially decrease the severity of disease caused by pathogens, their comparatively short reproduction times allow them to evolve and rapidly respond to the changing climactic conditions, ultimately leading to an increased volume of outbreaks (Anderson et al., 2020; Velásquez et al., 2018). The diseases caused by these pathogens not only result in significant losses in the quantity and quality of crop yields but also contribute to the increased cost of agricultural practices through the use of chemicals and other mitigation tactics and cause downstream impacts on human health, including the loss of nutritious food (Chaudhry & Sidhu, 2022; Ristaino et al., 2021). Of these plant pathogens, fungi are the greatest threat to food security as they often cause diseases in cereal crops which comprise 32% of the global food supply (FAO, 2021; Savary et al., 2019; Wing et al., 2021). Given the significant risk emerging pathogens pose to food security and human health, understanding how the changing environment impacts the

emergence and re-emergence of fungal pathogens is essential (Fones et al., 2020; Nnadi & Carter, 2021).

Emerging fungal pathogens are those that, in the past 30 years, have either increased in their geographic or host range, have significantly increased their infection rate, or have newly evolved (Anderson et al., 2004; Corredor-Moreno & Saunders, 2020; Nnadi & Carter, 2021; Ristaino et al., 2021). As the global average temperature continues to rise, the geographic range of fungal pathogens is expanding and causing disease outbreaks in areas where they have never been previously reported. For example, the rust fungus *Puccinia striiformis*, which causes stripe rust on wheat crops, previously showed a preference for colder climates but has recently expanded into warmer regions. Older *P. striiformis* strains have evolved into novel strains that are not only thermotolerant and can survive these warmer conditions, but are also more aggressive, allowing this fungus to spread and cause infection worldwide (de Vallavieille-Pope et al., 2018; Nnadi & Carter, 2021). Another disease that causes devastation across cereal crops is *Fusarium* head blight, caused by members of the *Fusarium graminearum* species complex. Before global average temperatures increased, *Fusarium culmorum* was the primary species that infected crops in temperate regions as it prefers a cool, wet climate. However, since 2000, there has been a shift in the fungal species that causes infections in these temperate regions from *F. culmorum* to *Fusarium graminearum* - which typically prefers a warm, humid environment. As *F. graminearum* shifts into these temperate regions, it is not only causing a greater loss in crop yield due to its more aggressive infection rate, but it also produces more mycotoxins which can be harmful to both human and animal health. To make matters worse, the production of mycotoxins increases when this fungus is exposed to temperature and water stress, both prominent abiotic stressors caused by the changing climate (Magan et al., 2011;

Nnadi & Carter, 2021). As fungal pathogens are responsible for 30% of emerging plant diseases that threaten human health and food security, there is a growing need to understand how the environmental pressures will impact the survivability of these pathogens and the severity of their diseases (Anderson et al., 2004; Corredor-Moreno & Saunders, 2020).

Investigations into the stress responses of fungi have primarily focused on functionally characterizing genes involved in stress response pathways. For example, in *Saccharomyces cerevisiae*, genes involved in the high osmolarity glycerol (HOG) and mitogen activated protein kinase (MAPK) pathways have been widely studied and the conservation of these pathways has been explored across other fungi (Nikolaou et al., 2009). However, given the understanding that non-coding RNAs (ncRNAs) are responsible for a wide range of regulatory roles, novel investigations into ncRNAs could further elucidate the mechanisms by which fungi adapt to and survive these changing environmental conditions (Wight & Werner, 2013). To gain a better understanding of the potential roles ncRNAs play in fungal stress response, this thesis focused on exploring a subset of ncRNAs, known as natural antisense transcripts (NATs) and investigated their roles in modulating the stress response of the model fungal plant pathogen *Ustilago maydis*.

CHAPTER TWO: LITERATURE REVIEW

2.1 Fungal plant pathogens

Fungi are a highly diverse kingdom that diverged approximately 1 billion years ago and are responsible for essential functions within virtually all environments and ecosystems (Hawksworth & Lücking, 2017; Naranjo-Ortiz & Gabaldón, 2019; Peay et al., 2016). Although it is highly debated amongst mycologists, recent predictions estimate that there are between 2.2 and 3.8 million fungal species, of which only 120,000 are currently known (Hawksworth & Lücking, 2017). Most of these known fungal species are saprophytes, which are responsible for promoting homeostasis in ecosystems through their ability to recycle nutrients (Fisher et al., 2020; Lucca, 2007). However, as of 2020, over 8,000 fungal species have been identified as causing diseases in plants and as the climate continues to change, the number of disease causing fungi are expected to rise (Fisher et al., 2020; Koeck et al., 2011).

Fungal plant pathogens are traditionally split into three groups based on their method of nutrient uptake. First, necrotrophic pathogens cause necrosis and tissue death in infected plants and extract nutrients from the dead tissue to support their growth (Doehlemann et al., 2017; Gebrie, 2016). Alternatively, biotrophic pathogens rely on nutrient uptake from living cells of their host plants and must maintain their host viability to sustain fungal growth. Finally, hemibiotrophic pathogens combine both strategies by exploiting a biotrophic phase to infect the plant and then transitioning into a necrotrophic phase where cell death is induced (Doehlemann et al., 2017; Gebrie, 2016; Lanver et al., 2018). Although biotrophic plant pathogens can often be mistaken as less harmful compared to their counterparts, they are responsible for some of the most economically destructive plant

diseases, including stripe rust on wheat (*Puccinia striiformis*) which causes an estimated $979 million decrease in wheat production worldwide (Lorrain et al., 2019; Mapuranga et al., 2022).

2.2 Biotrophic plant – pathogen interactions

The host plants of biotrophic fungal plant pathogens are often the greatest drivers of evolution the pathogens face since pathogens rely on their hosts for not only their source of nutrients but also the completion of their life cycle (Doehlemann et al., 2017; Möller & Stukenbrock, 2017). Part of this evolution is due to the inherent nature of the host plant to mount physical and chemical defence mechanisms in response to infection and colonization by the pathogen (Möller & Stukenbrock, 2017). As the host evolves novel systems to detect and defend against pathogens, the pathogens themselves evolve new mechanisms to surpass and suppress the host's defences, ultimately resulting in a co-evolutionary relationship (Doehlemann et al., 2017; Möller & Stukenbrock, 2017; Rausher, 2001; Torres et al., 2020).

Plants have evolved several sophisticated strategies to defend against the invasion and growth of biotrophic plant pathogens. The main system is the plant innate immune response which includes the pathogen associated molecular patterns (PAMP)-triggered immunity (PTI) and the effector-triggered immunity (ETI). PTI is activated when a pathogen interacts with extracellular pattern-recognition receptors in the host cell's plasma membrane (Gebrie, 2016; Velásquez et al., 2018). When the pathogen is detected, multiple defence mechanisms can be initiated, including the expression of defence genes and hormones, strengthening of the cell wall, and the production of reactive oxygen species

(ROS). Although PTI can protect against most microbes the plant encounters in its environment, the low specificity of the recognition system and weak signaling can allow biotrophic pathogens to adapt to this response and secrete effectors that suppress the PTI and allow for the successful infiltration of the host (Gebrie, 2016; Mapuranga et al., 2022; Velásquez et al., 2018). This is where ETI plays a major role in plant defence systems. When a plant resistance protein detects a pathogen effector, a signaling pathway is triggered, and a cascade of disease defences ensues. After the initial recognition of the pathogen effector, defence mechanisms are triggered, which include the production of ROS, protein phosphorylation, phytohormones, and, if all else fails, programmed cell death (Gebrie, 2016; Velásquez et al., 2018). Although plant defence mechanisms are sophisticated, biotrophic fungi have developed several mechanisms to evade plant immune defences.

To survive in a host plant, fungal pathogens must suppress and manipulate the host's defence system, which often begins with the secretion of molecules that counteract the initial immune response. For example, when plants sense a pathogen, one of their first responses is the production of ROS; so, if a pathogen is to survive in this environment, they must counteract and detoxify these ROS (Pradhan et al., 2021). Another approach to surviving plant immune responses is by evading recognition. To successfully evade detection, pathogens have evolved putative effectors designed to surpass the host's defences. Biotrophic fungi also utilize infection structures, such as appressoria, which allow for direct infection of epidermal plant cells aided by the secretion of plant cell wall degrading enzymes (Gebrie, 2016; Lanver et al., 2018). Although there is a general understanding of the basic concepts that allow these fungi to adapt to and survive their

host's defence systems, the specific machinery that the pathogens exploit is still under investigation (Mapuranga et al., 2022).

Although the host plants have the greatest impact on the evolution of biotrophic fungal plant pathogens, these interactions do not occur in isolation. As the climate changes, the alterations in the interactions between hosts and their pathogens emphasize the role that environments play in disease development. For disease to occur, there must be a susceptible host, a virulent pathogen, and a favourable environmental condition (Scholthof, 2007; Velásquez et al., 2018). Although the favourable environment may change depending on the specific host and pathogen, a deviation from the preferred environment can lead to an increase, decrease, or no change in disease development. Environmental conditions that ensure a favorable infection rate include temperature, water level, CO_2 concentration, soil condition and nutrient availability. As the climate continues to change, all these various factors have the potential to be altered, and there is already evidence of the negative impact these changes are having on plant defence systems. For example, in *Arabidopsis* and bean plants, altered water and humidity levels have caused a decline in the efficiency of the PTI. Under normal conditions, stomata in the stems and leaves are triggered to close when the PTI detects a pathogen. However, when faced with high humidity, stomatal closure by the PTI is blocked, and the plants are left open for further infection and increased disease severity (Velásquez et al., 2018). Additionally, as the global average temperatures rise, several plants have experienced a deterioration in their ETI systems, and in some cases, they have been fully compromised. For example, in tobacco and tomato plants, when temperatures reach above 30°C, they cannot elicit an effective ETI response upon infection by a biotrophic pathogen (Velásquez et al., 2018).

Adaptive mechanisms of fungal pathogens allow them to survive and exploit the changing climactic conditions. Prior to the rise in global temperatures, fungal pathogens faced dramatic reductions in population size, and the associated infection rate, due to low temperatures in the winter months (Santini & Ghelardini, 2015). However, as climate change continues, milder winter temperatures result in increased overwintering and, as a result, increased disease severity (Santini & Ghelardini, 2015; Velásquez et al., 2018). The presence of milder winters also promotes fungal pathogen evolution, as the reproduction rate of plant pathogens is tightly linked to temperature and moisture. The altered temperature and rainfall patterns associated with climate change have caused an elongation of the growing season which provides ample time for pathogen reproduction and dissemination, thereby resulting in an increased rate of evolution (Santini & Ghelardini, 2015). Although alterations in the climate are not always favourable for pathogens, biotrophic pathogens' relationship with their hosts has, in some ways, better prepared them to survive the changing environmental conditions.

2.3 Fungal stress responses

To survive, all cells must sense and react appropriately to changes in their environment. As fungal plant pathogens evolve, they rely on their ability to detect changes in their host plants to survive and exploit weaknesses in the plant's defence system, which facilitates successful infection (Newton et al., 2011). This evolution includes developing a stress response system known as an anticipatory protective response (Pradhan et al., 2021). These responses are also known as adaptive prediction and have evolved in pathogens that

experience predictable environmental changes, such as those experienced as part of a host's defence system (Brown et al., 2017; Pradhan et al., 2021).

At the center of adaptive prediction is the classic response to environmental stress, controlled by conserved stress response mechanisms (Pradhan et al., 2021). The foundation of our understanding of these stress response mechanisms is primarily based on studies performed on *Saccharomyces cerevisiae* and *Schizosacchromyces pombe,* which mainly focused on their response to individual stresses. These studies discovered key stress response mechanisms for various environments, including those caused by oxidative, osmotic, and nutrient stressors. When exposed to oxidative stress, fungi modulate their response using AP-1-like transcription factors and response regulators. In *S. cerevisiae*, Yap1 from the AP-1 family is the transcription factor central to the regulation of approximately 500 genes involved in this stress response (Fausto et al., 2019; Molina & Kahmann, 2007; Pradhan et al., 2021). Orthologs of Yap1 have been discovered in *S. pombe* and *Kluyveromyces lactis,* as well as in pathogenic fungi including *Cochliobolus heterostrophus, Candida albicans,* and *Ustilago maydis* (Enjalbert et al., 2006; Molina & Kahmann, 2007; Pradhan et al., 2021). Although there is conservation of these AP-1-like transcription factors across both pathogenic and non-pathogenic fungi, the mechanisms that activate these transcription factors vary. This indicates that although the stress pathways are conserved, links between them have diverged (Pradhan et al., 2021).

Upon exposure to osmotic stress, a group of evolutionarily conserved stress-activated protein kinases, including Hog1 in *S. cerevisiae*, Sty1 in *S. pombe* and SakA in *Aspergillus fumigatus* work to maintain osmohomeostasis (Brown et al., 2017; José De Assis et al., 2018; Pradhan et al., 2021). In pathogenic fungi, such as *C. albicans*, the signaling of the Hog1 and SakA conserved pathways not only promote resistance to

osmotic stress but also influence virulence factors that impact the pathogenicity of the fungus. Additionally, genome-wide transcriptional profiling studies of *S. cerevisiae* revealed a core set of genes that were upregulated when the fungus was exposed to various stressors, including heat, oxidative, osmotic, and nutrient stress. Upon identification, this group of genes was called the core stress response (CSR), and the signaling of this response is mediated by the activation of Msn2 and Msn4 transcription factors as well as protein kinase A (PKA) signaling pathways (Causton et al., 2001; Gasch et al., 2000). Additional genome-wide transcriptional profiling studies performed on *Candita glabrata, A. fumigatus, Cryptococcus neoformans,* and *S. pombe,* revealed that, although these fungi are evolutionarily diverse, they all contain a CSR (Brown et al., 2017; Pradhan et al., 2021).

The energetic demand that comes with activating CSRs that can contain upwards of one hundred genes indicates that these systems likely evolved over time. A leading theory surrounding the development of CSRs is based on adaptive prediction, the fungi's ability to predict impending environmental changes. Adaptive prediction evolved from the concept of stress cross-protection, the exposure of fungi to a non-lethal dose of one stress provides protection to the subsequent exposure of another unrelated stress (Brown et al., 2017; Pradhan et al., 2021). The use of *S. cerevisiae* in breweries is a clear example of adaptive prediction. During the fermentation process, there is a rise in temperature, followed by a transition from fermentative growth to respiratory growth, which results in the exposure of *S. cerevisiae* to heat stress followed by oxidative stress (Brown et al., 2017; Pradhan et al., 2021). The predictability of this sequential exposure to stress allowed for the rapid evolution of an anticipatory protective response. The accumulation of multiple anticipatory protective responses is thought to be the foundation upon which these CSRs evolved.

In pathogenic fungi, it is hypothesized that there are anticipatory protective responses that have evolved to assist in the evasion of a host's immune response and the subsequent infection of the host. However, unlike in the CSRs which are thought to have evolved as a response to environmental stress, there is a lack of phylogenetic clustering of these mechanisms that protect against impending immune attack (Pradhan et al., 2021). For example, some pathogenic *Candida* species, have hypoxia-induced β-glucan masking. However, there is no clear relationship between the development of this phenotype and phylogeny. This lack of phylogenetic clustering suggests that these anticipatory responses have evolved relatively recently in response to alterations in selective pressures (Pradhan et al., 2021). The ability of fungi to rapidly evolve these anticipatory protective mechanisms to better survive alterations in selective pressures suggests that fungal plant pathogens may be better equipped to adapt to and survive the changing climate compared to their hosts.

2.4 *Ustilago maydis*

Ustilago maydis is a basidiomycete biotrophic plant pathogen that causes tumor development on all aerial parts of its host plant, maize (*Zea mays*). This fungus belongs to a group of plant pathogens known as the smut fungi, which include over 1600 fungal plant pathogens, some of which cause considerable losses in cereal crops (Doehlemann et al., 2008; Flor-Parra et al., 2007; Goulet et al., 2020). Since *U. maydis* can be cultured in a lab, is amenable to molecular manipulation, and has a sequenced and annotated genome, it has been considered one of the top ten fungal models for scientific research (Kämper et al., 2006; Olicón-Hernández et al., 2019).

The life cycle of *U. maydis* (Figure 1) begins when non-pathogenic haploid cells that contain compatible mating-type alleles recognize each other and fuse on the surface of the host. The fusion of these haploid cells results in the start of the pathogenic portion of the life cycle through the formation of a dikaryotic filament which invades the host using specialized infection structures called appressoria (Doehlemann et al., 2008; Flor-Parra et al., 2007; Kämper et al., 2006; Lanver et al., 2014; Olicón-Hernández et al., 2019). After penetration, the fungus grows between and through the host plant's cells, manipulating the host's metabolism to obtain nutrients and resources to support its own growth (Redkar et al., 2017). In response to fungal infection, plant tumors develop, within which the fungus proliferates and differentiates to form dormant teliospores. When these tumors dry and crack, the teliospores can be dispersed and, upon germination, can form haploid sporidia, which initiates another round of this dimorphic life cycle (Donaldson & Saville, 2013; Kämper et al., 2006; Salmerón-Santiago et al., 2011).

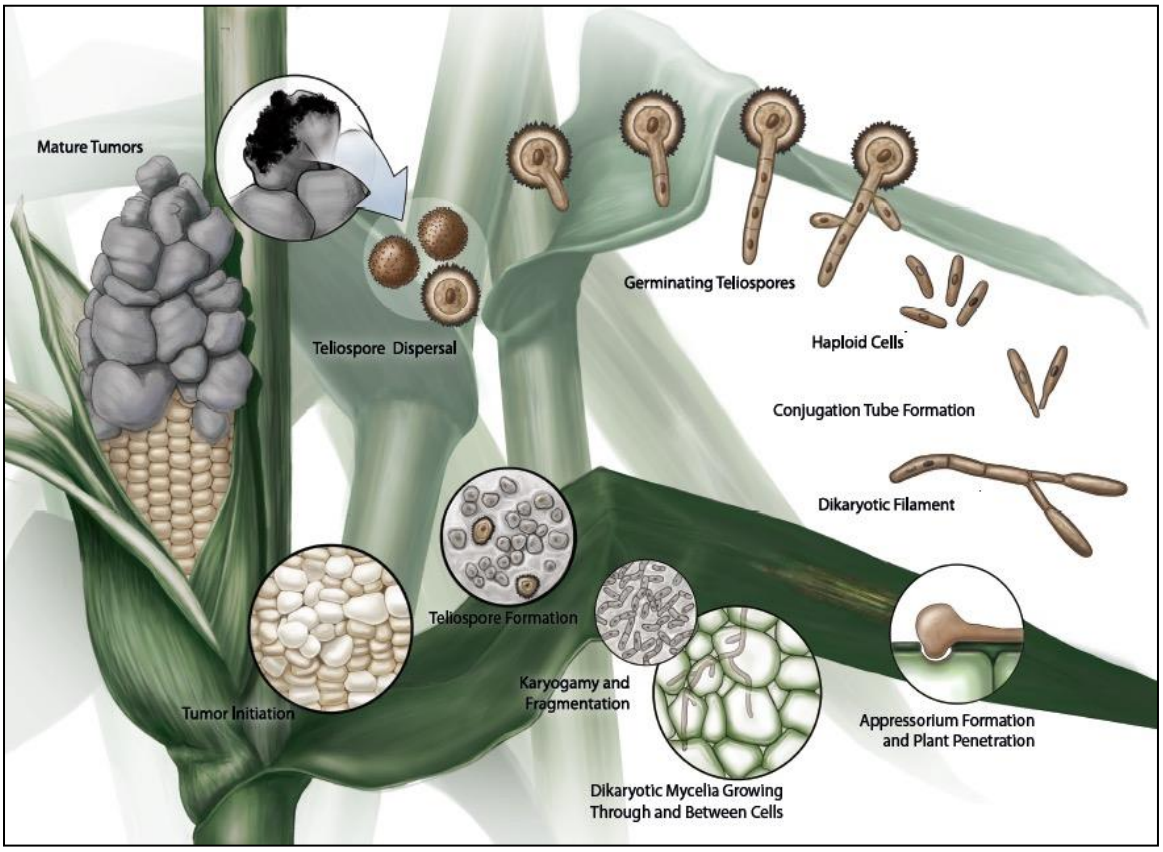

Figure 1. *Ustilago maydis* life cycle inside Zea mays. This figure was copied with permission from Saville *et al.* (2012).

Annotation of the *U. maydis* genome sequence created a better understanding of the pathogenic mechanisms used during infection (Liebal et al., 2022). After initial genome sequencing, which revealed a 20.5 Mb genome, additional expressed-sequence tag (EST) library investigations were performed to elucidate the annotation of protein-coding genes in *U. maydis* (Donaldson et al., 2017; Ho et al., 2007; Kämper et al., 2006). Before this analysis, the hypothesis surrounding how this fungus could efficiently suppress its host's immune defences and manipulate its host's metabolism was through the secretion of various effectors (Redkar et al., 2017). Upon analyzing the genome, over 700 candidate

effector proteins were defined, and further analysis revealed that 20% of these were found in 22 gene clusters, many of which are upregulated in times of biotrophic interaction. The functional characterization of several effectors involved in virulence has been completed, and roles in suppressing the defence system of the host plant during early infection have been confirmed (Kämper et al., 2006; Redkar et al., 2017). Additionally, annotation of the genome predicted potential genes encoding an RNA helicase (*UMAG_00282*), a histone H2A (*UMAG_01504*), a general transcriptional adaptor/co-activator (*UMAG_05213*), and a diacylglycerol pyrophosphate phosphatase (*UMAG_10421*) that have potential roles in various cellular processes including the response to abiotic and biotic stressors (Chen & Dent, 2021b; Coleman et al., 2001; Donaldson et al., 2017; Oshiro et al., 2003; Owttrim, 2006; Singh et al., 2021). Although analysis of EST libraries did aid in improving the understanding of protein-coding regions, it also identified hundreds of non-coding RNAs (ncRNAs), which are thought to have important regulatory roles (Donaldson et al., 2017). Previous analysis of ncRNAs in other organisms, including plants and fungi, revealed roles in regulating responses to abiotic and biotic stresses, paving the way for future analysis of ncRNAs' roles in the stress response of the model biotrophic fungus, *U. maydis*.

2.5 Natural antisense transcripts (NATs)

Non-coding RNAs are functional RNAs that lack protein-coding potential; in other words, they do not contain an open reading frame (as reviewed in Donaldson & Saville, 2012; Wang et al., 2017). Within this broad definition of ncRNAs, there are subcategories that divide these transcripts based on both their size and function. Short ncRNAs encompass all ncRNAs with less than 200 nucleotides and include short interfering RNAs, microRNAs,

and PIWI-interacting RNAs (as reviewed in Donaldson & Saville, 2012). Long ncRNAs (lncRNAs) encompass all ncRNAs that are greater than 200 nucleotides in length and often perform regulatory functions at both the transcriptional and post-transcriptional levels (as reviewed in Donaldson & Saville, 2012). Similar to mRNAs, lncRNAs are typically 5` capped and polyadenylated. A subset of ncRNAs are natural antisense transcripts (NATs), which have regions of their sequence complementary to that of an mRNA (Donaldson & Saville, 2012; Goulet et al., 2020; Li et al., 2021).

NATs were first discovered in bacteria in 1981 and have since been found in a wide range of eukaryotic organisms, including plants, fungi, and even humans (Wight & Werner, 2013). With the discovery of such a broad array of NATs came the further breakdown and classification based on their mode of action and orientation regarding their complementary mRNA. First, NATs can be classified as either divergent (overlap at 5` ends), convergent (overlap at 3` ends), fully overlapping, or embedded (as reviewed in Donaldson & Saville, 2012; Wight & Werner, 2013). Additionally, NATs can be classified based on whether they act in *cis* or in *trans*. *Cis*-acting NATs primarily exploit regulatory roles that act on their corresponding mRNA. Whereas *trans* NATs can execute regulatory functions on transcripts at other loci (Wight & Werner, 2013). Although it is widely accepted that both *cis* and *trans*-acting NATs regulate gene expression, most research is focused on exploring the mechanisms of *cis*-acting NATs (Li et al., 2021).

There is still limited information regarding the function of NATs in fungi, but it is generally understood that they can regulate the expression of target genes, whether in *cis* or *trans* (Li et al., 2021). For example, studies performed on *S. cerevisiae* revealed functional roles of NATs in regulating gene expression through transcriptional interference, chromatin remodeling, and double-stranded RNA formation (Donaldson & Saville, 2012;

Harrison et al., 2009; Tisseur et al., 2011). Further investigation of the function of NATs was performed in *U. maydis,* which revealed novel roles in modulating protein and gene expression, controlling RNA stability, and influencing mitochondrial function and disease development (Donaldson & Saville, 2013; Morrison et al., 2012; Ostrowski & Saville, 2017).

Comparative transcriptome analysis of three related smut fungi, *U. maydis, U. hordei,* and *Sporisorium reilianum,* revealed that of the 2617 NATs in *U. maydis*, 349 are conserved among all three species (Donaldson et al., 2017). The conservation of NATs among these smut species suggests that not only do they have functional roles but that these NATs likely exert their functions without the RNA interference (RNAi) pathway, since genes involved in RNAi are not present in *U. maydis* (Donaldson et al., 2017; Laurie et al., 2008, 2012). Additionally, differences in the expression levels of NATs across various cell types indicate potential roles in modulating gene expression in different developmental stages and environmental conditions (Donaldson & Saville, 2013; Goulet et al., 2020). Recent studies have focused on the potential role of NATs in various stress environments. For example, when *S. cerevisiae,* a fungus that does not have a functioning RNAi pathway was exposed to osmotic stress, a NAT complementary to the CDC28 gene regulated the expression of its complementary mRNA through chromatin remodeling (Li et al., 2021). Similarly, when *S. pombe,* a fungus that does have a functioning RNAi pathway was exposed to oxidative stress, a stress-response transcription factor, which regulates the CSR, was found to be reduced when its complementary NAT levels were increased (Leong et al., 2014; Li et al., 2021). The novel discovery of NAT involvement in the regulation of the CSR emphasizes the need for future research that explores the potential roles these transcripts have in the stress response of fungi.

2.6 Research objectives

There is a general understanding of how fungal stress responses have evolved, but there are still a lot of knowledge gaps surrounding fungal stress signaling pathways and the mechanisms controlling their stress responses. The research presented in this thesis focused on elucidating stress response mechanisms in the fungal plant pathogen *U. maydis* through three objectives, including: 1) identifying NATs that had altered expression levels in stress environments, 2) expressing the identified NATs to determine if there is a stress related phenotypic response, and 3) determining if the expression of the NAT impacts its complementary mRNA. By focusing on the potential role that NATs play in the stress response of the model fungus *U. maydis*, this research attempts to gain a better understanding of the various transcriptional and post-transcriptional processes that assist in regulating stress response pathways.

CHAPTER THREE: MATERIALS & METHODS

3.1 Strains and growth conditions

The fungal strains used in this study are listed in Table 1. *U. maydis* strains were grown on PDB (2.5% w/v potato dextrose broth; BioShop) supplemented with 2% w/v agar (Fisher Bioreagents) for three days at 28°C. Single colonies were inoculated into liquid minimal media (MM; 0.3% w/v potassium nitrate, 6.25% v/v salt solution, pH 7.0) supplemented with 1% v/v D-glucose (BioShop) and grown for 3 days at 28°C, 250 rpm unless otherwise specified. All fungal strains were stored at -70°C in 15% v/v glycerol.

For experiments involving exposure to stressed environments, four stress conditions were created by modifying the minimal media recipe. For the oxidative (OX) condition, 2 mM of H_2O_2 was added to MM, for the osmotic (OS) condition, 1 M NaCl was added to MM, and the minus nitrogen (MN) and minus carbon (MC) conditions were completed as described in Ho *et al.* (2007).

For RNA isolations of *U. maydis* strain 521 exposed to single stressors, haploid cells were grown in 6 mL of MM. The optical density (OD) of the cell culture was measured using Genesys^{TM} 10s Vis Spectrophotometer (ThermoFisher Scientific) at 600 nm. Once the OD_{600} reached 1.0 ± 0.1, five flasks containing 250 mL MM were inoculated with 1 mL of the starter culture and grown at 28°C, 250 rpm for five days. After five days, the cells were pelleted by centrifugation at 3,000 x *g* for 15 min and the liquid was aspirated. Cells were then washed with 100 mL sterile dH_2O, centrifugation was repeated, and liquid was aspirated once more. To ensure a uniform concentration of cells were inoculated into each stress condition, 50 mL of dH_2O was added to each culture and the cultures were combined. Finally, 50 mL of the combined culture was transferred to each flask containing 200 mL of

either one of the four stressed conditions (OX, OS, MN, MC), or the MM control. Upon making the 200 mL of each condition, the concentration of ingredients in the media was adjusted so that when the additional 50 mL of the culture was added, the concentration of the media would be equivalent to what is expected for 250 mL. These cultures were grown for 12 hrs at 28°C, 250 rpm and then the cells were harvested immediately by pelleting.

For RNA isolations of *U. maydis* strain 521 exposed to staggered stressors, haploid cells were grown in 6 mL MM. Upon reaching an OD_{600} of 1.0 ± 0.1, three flasks containing 250 mL MM were inoculated with 1 mL of the starter culture and grown at 28°C, 250 rpm for five days (1.0 ± 0.1 OD). The cells were then pelleted, washed, and combined as previously outlined and 50 mL of the combined culture was transferred to each of three flasks, two containing 200 mL MN and one containing 200 mL of MM. The concentration of the ingredients within the 200 mL of media was once again adjusted so that the addition of the 50 mL of culture would result in a final concentration of the media expected for 250 mL. These cultures were grown for 12 hrs at 28°C, 250 rpm. Upon completion of the 12 hr growth, the cells were once again pelleted and washed with dH_2O. After the wash, one of the two cultures exposed to MN was resuspended in 250 mL OX media while the other was resuspended in 250 mL OS media. The cells grown in the MM control were resuspended in 250 ml MM. These cultures underwent another 12 hr growth at 28°C, 250 rpm and upon completion of this growth cycle, the cells were harvested immediately by pelleting.

For generation of competent protoplasts, a single colony of *U. maydis* 521 haploid strain was inoculated into 5 mL PDB and grown at 28°C, 250 rpm overnight. The following day, 100 µL of the overnight culture was inoculated into 100 mL YEPS (1% w/v yeast extract, 2% w/v peptone, 2% w/v sucrose; BioShop) and grown overnight at 28°C, 250

rpm. Transformed protoplasts were spread onto YEPS agar medium supplemented with 1 M sorbitol (BioShop), 2% w/v agar, and 250 µg mL^{-1} Hygromycin B (Hyg) and incubated at 30°C, for 4-5 days. For growth of 521 antisense expressing strains, PDB agar medium and MM liquid were supplemented with 250 µg mL^{-1} Hyg and grown for four days on solid agar medium and four days in 6 mL liquid. Antisense expressing strains, listed in Table 1, were stored permanently at -70°C as previously indicated.

DH5α *Escherichia coli* strains were grown on Luria broth (LB; EMD Millipore) supplemented with 100 µg mL^{-1} ampicillin (amp; BioShop) and 2% w/v agar at 37°C for 16-18 hrs. Single colonies were inoculated into liquid LB containing 100 µg mL^{-1} amp and incubated at 37°C, 250 rpm for 16-18 hrs.

Table 1. Strains used in this study

Haploid Strain	Relevant Genotype	Source
521[a]	*a1 b1*	Holliday, 1961
521[pCM768]	*a1 b1 [pCM768]*	This work
521[pCMas-*UMAG_00282*]	*a1 b1 [pCMas-UMAG_00282]*	This work
521[pCMas-*UMAG_01504*]	*a1 b1 [pCMas-UMAG_01504]*	This work
521[pCMas-*UMAG_05213*]	*a1 b1 [pCMas-UMAG_05213]*	This work
521[pCMas-*UMAG_10421*]	*a1 b1 [pCMas-UMAG_10421]*	This work

[a] Reference strain used for genome sequencing

3.2 Liquid growth and plate assays

For liquid growth assays, *U. maydis* haploid cells were grown in 5.0 mL of MM. Cells were pelleted by centrifugation at 5,000 rpm for 60 sec, the liquid was aspirated, and the cells were washed with 1.0 mL dH_2O. The centrifugation was repeated, the liquid

aspirated, and the cells were resuspended in dH_2O to a final concentration of 1.0 OD_{600}. When determining the growth rate in different concentrations of oxidative stress, 500 µL of the haploid strain at 1.0 OD was transferred to each of four flasks containing 50 mL of OX at different concentrations of H_2O_2 (0.0, 0.5, 1.0, 2.0 mM). OD_{600} measurements were recorded every 12 hrs for 120 hrs to determine the impact the various concentrations had on *U. maydis* growth rate. Three biological replicates were performed, and the significance of the growth rate differences was assessed by performing a Wilcoxon matched pairs test.

For plate assays of *U. maydis* strain 521, haploid cells were grown in 3.0 mL of MM. Cells were pelleted by centrifugation at 5,000 rpm for 60 sec, the liquid was aspirated, the cells were washed twice with filter sterilized dH_2O and resuspended in 200 µL dH_2O at a final concentration of 1.0 OD_{600}. The cell cultures were serially diluted to 1x, 10x, 100x, 1,000x, and 10,000x, with filter sterilized dH_2O, and 10 µL of each dilution was spotted on solid media made of MM, OX, OS, MN, and MC. For plate assays of the antisense expressing *U. maydis* strains, cells were grown in 3.0 mL of MM supplemented with 250 µg mL^{-1} Hyg. The cells were washed, resuspended, and serially diluted as previously indicated and 5 µL of each dilution was spotted on MM, OX, OS, MN, MC, agar medium all of which were supplemented with 250 µg mL^{-1} Hyg. Plate assays were incubated at 28°C and growth was assessed after five days. All plates were visualized and photographed on a Geliance 600 Imaging System (Perkin Elmer) and colonies were visualized on day five using a Leica S8 APO microscope (Leica Microsystems). All plate assays had both technical and biological replicates performed in triplicate.

3.3 Microscopy

Upon completion of the plate assays, cells from the 1x dilution spots were resuspended in 50 µL dH_2O and 5 µL was placed onto VWR VistaVision glass microscope slides (75x25x1 mm) and covered with a 1-ounce VWR microcover glass coverslip (18x18 mm) Microscopic observations of cell morphology were visualized using the Zeiss Axio Scope.A1 microscope (Carl Zeiss AG) at 100x and 400x magnification. Samples were observed with differential interference contrast (DIC) lighting and photographs were taken with an Axiocam 208 color camera (Carl Zeiss AG).

3.4 Primer and probe design

All primers (Table 2) were designed using Primer3, following the protocol outlined in Ho *et al.* (2010) and ordered from Sigma-Aldrich unless otherwise specified. For reverse transcription-PCR (RT-PCR), first strand synthesis primers were designed to target the 3` end of the antisense to ensure the synthesis of the longest possible cDNA template. For RT-qPCR a tagged primer system described in Donaldson and Saville (2013) was utilized to eliminate the occurrence of false priming. This 'tagged' primer had a set of nucleotides on the 5` end of the primer that are not complementary to the *U. maydis* genome. Upon using these 'tagged' primers for first-strand synthesis, this new sequence or 'tag' was incorporated into the cDNA. Primers complementary to the tags were used for qPCR amplifications. The Integrated DNA Technologies (IDT) primer and probe designing software, PrimerQuest, was used to design the qPCR primers and probes for both antisense and sense. All qPCR primers and probes were ordered from IDT.

Table 2. Primers used in this study

Primer	Nucleotide Sequence (5` to 3` direction) [a, b]	Tm (°C)
Strand-specific first strand synthesis		
umgapd_FS	CCGGGATGACGACCTTCTTG	
x1-um00282-FSS	GACGGTGTTTCTTGGTTGGG	
x1-um00592-FSS	CGTCGAAAAGAAACAGGCAG	
x2-um00592-FSS	CGTCTTCGTATACCACCTGT	
x1-um00685-FSS	CGTCACCCCGAAGAAAGAC	
x1-um00753-FSS	CGGTGAAGAAGAGTAACGGT	
x1-um00964-FSS	CGACGATGATGATGATGACG	
x2-um00964-FSS	CTCCTGTGTGCTCGTTTG	
x1-um01421-FSS	GGTTCAGTGTCTCGTCTAGG	
x1-um01504-FSS	GTCGTATCCACCGTCTCTTG	
x1-um01869-FSS	TGGCCAAGGTGAGCTGTTTA	
x2-um01869-FSS	CTGCTACTGTCCAAGGATCG	
x1-um02490-FSS	CACCAATCCGACGCCAAC	
x2-um02490-FSS	TCGGAGAATTTGCACGTTACA	
x1-um03307-FSS	CATGGCGGTAAATCGATGGG	
x2-um03307-FSS	GGCTAATTCGGCGAAGTTAGG	
x1-um05213-FSS	TGGGCAAAGTGTGGGATTTC	
x2-um05213-FSS	GCATCCCAGAGTCCTAGCAA	
x1-um05600-FSS	TTCGTCCGCAAAGCAGT	
x2-um05600-FSS	GCTCTGGAAATGCAACTGGT	
x1-um06063-FSS	CGAGCTGATCTGTTTTGGCA	
x1-um10421-FSS	GAAGATGGTGAGGCGAGGTA	
x1-um00239-FSS	CGACCAAGGAGATTCGCAAG	
x2-um00239-FSS	GCTGCATCTTGGGTTTGGAT	
x1-um00903-FSS	ATCGTCGCTTCCATGGTTTG	
x2-um00903-FSS	GCGTACCAGCTGTGTTACAA	
x1-um01891-FSS	TCAACCTCATCGACTGTCCC	
x1-um03501-FSS	TGGACCAGCTCAAGTTGATG	
x1-um10450-FSS	GCCACCTACAGCGATACAG	
RT-PCR		
umgapd_F	CATAATGTCTCAGGTCAACATCG	58
umgapd_R	GGATGTTGGAGGGGTCCT	58
x1-um00282-F	TGCTGTCGTTTGGCTCCT	58
x1-um00282-R1.2	TGTTTCTTGGTTGGGCTACAC	58
x1-um00592-F2	CTTGCTTGCTTCGCCATT	58

x1-um00592-R2	AAAAGAAACAGGCAGCCAAG	58
x2-um00592-F2	TCATCAACACCGAGGCTAAG	58
x2-um00592-R2	GGAACAATGCACGTCTTCG	58
x1-um00685-F	CGCTTCTTTCGCTCCTCC	60
x1-um00685-R	TCACCCCGAAGAAAGACGAC	60
x1-um00753-F1.2	CGCTGTTGTCAACGGTTTAG	58
x1-um00753-R	ATGTTGGGTGGTCAAGTTGA	58
x1-um00964-F2	TTTCCTTGCTCTTTGGTTCG	58
x1-um00964-R2	AAACGCAAAGCCGAAAACTA	58
x2-um00964-F	CTTGTGCGTGTCTTGTTGAT	58
x2-um00964-R1.2	CGTACAACCGCCAGACCT	58
x1-um01421-F1.2	GTCTGGTCTCCCCATTCGT	58
x1-um01421-R	GAGAGTGTGTGGGGAGATTC	58
x1-um01504-F1.2	ATACCTCGGTCAGTCGGATT	58
x1-um01504-R	ACCGTCTCTTGCGAAAGG	58
x1-um01869-F1.2	GAGCATGGTTGGGTGGTC	58
x1-um01869-R	CTAGGCACGACGAAGAGGAT	58
x2-um01869-F1.2	GCAGCGACGGGCAAAGTT	58
x2-um01869-R	TACTGTCCAAGGATCGGGT	58
x1-um02490-F2	ACGGAATCAACTTGCCCTTA	58
x1-um02490-R2	AACTCACCAACGCATCGAC	58
x2-um02490-F	GAGGTTGGGCAGCAATAGGT	59
x2-um02490-R1.2	CCGTAAGCAACAGAAAAAGCA	59
x1-um03307-F	TAACCTTTGCCGTGACCCAA	59
x1-um03307-R	ACCTATGCTGACGGAACCAT	59
x2-um03307-F1.2	CTGGTCCCAATGCTACCCTA	59
x2-um03307-R	TCGGCGAAGTTAGGTTCTGA	59
x1-um05213-F	CTCTTCCGAACAGTCCACCT	58
x1-um05213-R1.2	GGTTGGCTGGATAGCAACAT	58
x2-um05213-F2	GTATGCGAGCAAGCGATACA	58
x2-um05213-R2	CAGCATCCCAGAGTCCTAGC	58
x1-um05600-F1.2	AGCCAGAGGGGAAACCAG	58
x1-um05600-R	GTCCGCAAAGCAGTCAGT	58
x2-um05600-F2	GCATACCGCCAAGATACAGG	59
x2-um05600-R2	TGACAAGGCTAGAGGGTTGC	59
x1-um06063-F2	CAAGTTCAGCGTGGGTTTG	58
x1-um06063-R2	GCTGATCTGTTTTGGCATTG	58
x1-um10421-F1.2	GACGCATGGTGTGAAGGTC	59
x1-um10421-R	ACAATCTTACCCACGGCAAC	59
x1-um00239-F1.2	AGTCAACGTCCTCGAACCTC	60
x1-um00239-R	GGAATTTTGCCAAACACGCC	60
x2-um00239-F1.2	CCCTCTGCTCACTCCTCTTC	59
x2-um00239-R	TCTTGGGTTTGGATATGGACC	59

x1-um00903-F2	GAACCTCTTGAGCTGGATGC	59
x1-um00903-R2	AAAAGTTGGGCAACAACGAC	59
x2-um00903-F1.2	TCATCCTGATTCTTGCGTTT	58
x2-um00903-R	GCACATAGGCAAGCGGATAC	58
x1-um01891-F2	GCCCAGAATTTCCTCCATCT	59
x1-um01891-R2	GCCAAGCAGAAGAACCTGAC	59
x1-um03501-F2	GCGGTTCGACACGACGAG	60
x1-um03501-R2	TGGACCAGCTCAAGTTGATGTA	60
x1-um10450-F	CTCTTCCTTTGCGGTACACT	58
x1-um10450-R	CATGGGAGTCTATGCGGATC	58

Tagged strand-specific first strand synthesis

x1-um00282_FS_Tag	cgaggatcatggtggcgaataaGACGGTGTTTCTTGGTTGGG
x1-um00282_S_FS_Tag_OL	cgaggatcatggtggcgaataaCCATTTTGGCTTCGACGAG
x1-um01504_FS_tag	cgaggatcatggtggcgaataaGTCGTATCCACCGTCTCTTG
x1-um01504_S_FS_Tag_OL	cgaggatcatggtggcgaataaGAACGGCGGCGAGGTAGA
x1-um05213_FS_Tag	cgaggatcatggtggcgaataaTGGGCAAAGTGTGGGATTTC
x1-um05213_S_FS_Tag_OL	cgaggatcatggtggcgaataaCGTGTCACCTCAAAGCTCTG
x1-um06063_FS_Tag	cgaggatcatggtggcgaataaCGAGCTGATCTGTTTTGGCA
x1-um06063_S_FS_Tag_OL	cgaggatcatggtggcgaataaCCGACATGAGTTTGGTAGCT
x1-um10421_FS_Tag	cgaggatcatggtggcgaataaGAAGATGGTGAGGCGAGGTA
x1-um10421_S_FS_Tag_OL	cgaggatcatggtggcgaataaCCGCACAGCTCTTTCAGAC

RT-qPCR

umgapd FWD Set 5	CCACCATCGAATCTTTCTTTCTC
umgapd REV Set 5	GGAAGACGATACGTCCGATAC
x1-um00282 FWD Set 1	CTGTCGTTTGGCTCCTAGATG
x1-um00282 REV Set 1	AGGATCATGGTGGCGAATAAG
x1-um00282_S FWD Set 5	GTATGACGTACGACGAGGTG
x1-um00282_S REV Set 5	CATGGTGGCGAATAACTTCTTG
x1-um01504 FWD Set 1	GACGGAGGAAGATCGAAAGATG
x1-um01504 REV Set 1	GAGGATCATGGTGGCGAATAA
x1-um01504_S FWD Set 1	GGTCGTATCCACCGTCTCT
x1-um01504_S REV Set 1	GAGGATCATGGTGGCGAATAA

x1-um05213 FWD Set 3	GCGTCAAAGTAGCCCATCT
x1-um05213 REV Set 3	GAGGATCATGGTGGCGAATAA
x1-um05213_S FWD Set 3	GCTCGCATACGATTGTCTACTT
x1-um05213_S REV Set 3	GAGGATCATGGTGGCGAATAA
x1-um06063 FWD Set 1	TCGGACGAGAGAAGCTAGAG
x1-um06063 REV Set 1	GAGGATCATGGTGGCGAATAA
x1-um06063_S FWD Set 2	GCTTCTCTCGTCCGAGCTTA
x1-um06063_S REV Set 2	ATGGTGGCGAATAATCTTTGGG
x1-um10421 FWD Set 1	AGTTTCCTGGAGCTTCGTTATC
x1-um10421 REV Set 1	AGGATCATGGTGGCGAATAAG
x1-um10421_S FWD Set 3	GACTTGGATACCGAGCATGAA
x1-um10421_S REV Set 3	GAGGATCATGGTGGCGAATAA

RT-qPCR TaqMan probes

umgapd PRB Set 5	/56-FAM/AACATCGGT/ZEN/ATCAACGGCTTCGGT/3IABkFQ/
x1-um00282 PRB Set 1	/56-FAM/TGTAGCCCA/ZEN/ACCAAGAAACACCGT/3IABkFQ/
x1-um00282_S PRB Set 5	/56-FAM/ATCTAGGAG/ZEN/CCAAACGACAGCAGC/3IABkFQ/
x1-um01504 PRB Set 1	/56-FAM/TTCGCAAGA/ZEN/GACGGTGGATACGAC/3IABkFQ/
x1-um01504_S PRB Set 1	/56-FAM/TGCGAAAGG/ZEN/GCAACTACGCTCA/3IABkFQ/
x1-um05213 PRB Set 3	/56-FAM/CGTTGAAGA/ZEN/AATCCCACACTTTGCCC/3IABkFQ/
x1-um05213_S PRB Set 3	/56-FAM/CTGGAACAT/ZEN/GGTTACTTTGCCAACACG/3IABkFQ/
x1-um06063 PRB Set 1	/56-FAM/CACCGAGGC/ZEN/AAGAACAATGCCAAA/3IABkFQ/
x1-um06063_S PRB Set 2	/56-FAM/CGGCAAACC/ZEN/CACGCTGAACTTG/3IABkFQ/
x1-um10421 PRB Set 1	/56-FAM/ACCGTTGCC/ZEN/GTGGGTAAGATTGTA/3IABkFQ/
x1-um10421_S PRB Set 3	/56-FAM/AACTACACC/ZEN/AAGCCAAGTGCTGGA/3IABkFQ/

Antisense expression vector creation

x1-um00282_F_BamHI	ggaggatccTTCGACGAGCTTCTTGACAC	63
x1-um00282_R_HindIII	ggaaagcttATCGCCTATCGCACTACGTC	63
x1-um01504_F_BamHI	ggaggatccCGTTACCGGCAAGTTCAAGA	65
x1-um01504_R_HindIII	ggaaagcttGTCTTCCGGTGGCAAGTCT	65
x1-um05213_F_BamHI	ggaggatccCAGCCTTCGCCTTTCCAC	64
x1-um05213_R_HindIII	ggaaagcttCCCTTCCTGCTGATCAAGTC	64
x1-um10421_F_SphI	ggagcatgcCAGGACATTGGGCCTATGAG	64
x1-um10421_R_HindIII	ggaaagcttTGCTAATGAGCAGCGGTATG	64
pgapd_79_F	GACCTCACTCTTCAAGAACAAGC	63

[a] Lower-case letters in primer sequences represent nucleotides not complementary to the *U. maydis* genome.
[b] Restriction endonuclease recognition cites are underlined.

3.5 Total RNA isolation, DNaseI treatment, reverse transcription, and transcript level analysis

U. maydis haploid cells were grown in liquid, pelleted by centrifugation, and the supernatant was removed. Total RNA extraction, precipitation, DNaseI treatment and genomic DNA contamination checks were performed as specified in Morrison *et al.* (2012). Haploid cell cultures were resuspended in TRIzol reagent and transferred to 2 mL screw-cap tubes containing Lysing Matrix C (MP Biomedicals). Cells were disrupted as described in Zahiri *et al.* (2005) and the RNA isolation was completed following the manufacturer's protocol for TRIzol reagent. A Nanodrop 8000 (ThermoFisher Scientific) was used to quantify total RNA and 15 µg of RNA was DNaseI (New England Biolabs) treated. Upon the removal of genomic DNA contamination, all treated RNA samples were normalized to 100 ng μL^{-1}.

First-strand synthesis reactions used 200 ng of DNaseI treated RNA as the template. Reverse transcription was carried out using the TaqMan® Reverse Transcription Reagents (Applied Biosystems) in 10 µL reactions following the conditions outlined in Morrison *et al*. (2012). RNA was primed with strand-specific primers (Table 2), oligo$(dT)_{16}$, or DEPC-treated H_2O which assessed the occurrence of false priming. In all reactions containing strand-specific primers, an internal control was included by adding a sense-specific *UMAG_gapdh* (*UMAG_02491*) primer. After reverse transcription, the resulting cDNA was diluted using 30 µL of DEPC-treated H_2O as specified in Ho *et al.* (2010).

All RT-PCRs were carried out using DreamTaq DNA polymerase (ThermoFisher Scientific) following the manufacturer's suggested protocol using the following conditions: 95°C for 10 mins, 35 cycles of [95°C for 30 sec, X°C for 30 sec, and 72°C for 1 min], 72°C for 10 mins and a 4°C hold. X°C corresponds to the annealing temperatures of the primers outlined in Table 2. One third of the product was separated electrophoretically on a 2% agarose gel (1x TAE) at 90 V for 75 min and visualized through ethidium bromide staining (0.3 µg mL^{-1}, EtBr; BioShop). Sizes were compared to a 50 bp ladder (Norgen Biotek).

Based on the RT-PCR results, select antisense were analyzed by RT-qPCR using TaqMan Universal PCR Master Mix (Applied Biosystems). Each reaction contained 4 µL sterilized dH_2O, 1 µL of 4 µM primer (forward and reverse), 2 µL of 2 µM TaqMan probe, 10 µL TaqMan Universal PCR Master Mix and 2 µL of cDNA template. All RT-qPCR reactions were run on a QuantStudio 3 (Applied Biosystems) using the following conditions: 50°C for 2 mins, 95°C for 10 mins, 40 cycles of [95°C for 15 sec and 60°C for 1 min], and a 4°C hold. Relative transcript levels for antisense and sense strands were calculated using the $2^{-\Delta\Delta CT}$ method outlined in Livak and Schmittgen (2001). Three technical replicates were performed for each sample and *UMAG_gapdh* was used as an endogenous control.

3.6 Identification of NATs of interest

This process started with the identification of 2617 NATs in *U. maydis* and the further discovery that 349 of these NATs were conserved amongst three related smut species, *S. reilianum, U, hordei,* and *U. maydis* (Donaldson et al., 2017). A literature search was performed on the genes complementary to these 349 NATs using a combination of google

scholar and the *Saccharomyces* Genome Database in September of 2019. This initial screen was used to determine if any of these genes had previous links to stress response. At the completion of this screen, 76 genes were identified. A secondary literature screen was performed on these genes in October of 2019 however, this time the previous ties to stress were limited to either oxidative, osmotic, nutrient, or an overarching general stress response. After the second literature screen, 30 genes remained. Finally, using data supplied by Donaldson *et al.* (2017), these genes were further limited based on their number of predicted antisense transcripts. Only genes with two or less predicted antisense transcripts were selected for further analysis. We selected a limiting factor of two predicted antisense as this allowed us to limit the number of NATs to an achievable number for screening using RT-PCR. Upon completion of these screens and my undergraduate thesis, 19 genes with a total of 28 antisense were selected for further analysis.

My graduate work began with RT-PCR screens performed on the 28 NATs to determine if any had altered levels in one of the stressed environments (OX, OS, MN, MC) compared to the control (MM). RT-qPCR was then performed on the NATs identified as having altered transcript levels to confirm and quantify the change in expression. NATs that were confirmed as having altered transcript levels in the single stressed environments of OX, OS, MC, and MN were selected for the creation of antisense expression constructs.

3.7 Creation of antisense expression constructs

To assess the impact antisense expression has on the stress response of *U. maydis*, four antisense transcripts were identified and selected to create antisense expression constructs using the *U. maydis* expression vector, pCM768. This is a non-integrating vector that

contains an autonomously replicating sequence (ARS), a Hygromycin-B resistance cassette (Kojic and Holloman, 2000), and it expresses transcripts inserted into the multiple cloning site by using the *U. maydis* promotor glyceraldehyde-3-phosphate dehydrogenase (Kojic and Holloman, 2000). To express antisense transcripts using this vector, the region of the genome complementary to the antisense transcripts of interest (sequences obtained from Donaldson *et al*., 2017) were amplified using PCR primers, which introduced restriction endonuclease recognition sequences at their 5` ends (Table 2).

Table 2 contains the specific primers, annealing temperatures (X°C), and restriction endonucleases (RE) used for the creation of each of the four antisense expression constructs. Amplification of the regions of interest were performed using Phusion® High-Fidelity DNA polymerase (ThermoFisher Scientific) following the manufacturer's protocol. Each reaction contained 27.5 µL of sterilized dH_2O, 10 µL of 5x Phusion Buffer, 4 µL of 2.5 mM dNTPs, 0.5 µL of 5 U μL^{-1} Phusion polymerase, 2 µL of 5 µM primers (forward and reverse), and 4 µL of 521 genomic DNA template. A GeneAmp™ PCR System 9700 thermocycler (Applied Biosystems) was used to run the reaction under the following conditions: 98°C for 30 sec, 35 cycles of [98°C for 10 sec, X°C for 10 sec, and 72°C for 30 sec], 72°C for 10 mins and a 4°C hold. The PCR product was analyzed by running 2 µL of the product on a 1.2% agarose gel (1x TAE) at 90 V for 1 hr and then visualizing it using EtBr (0.3 µg mL^{-1}). The sizes of the products were compared to FullRanger DNA ladder (Norgen Biotek). All PCR products were purified using the PureLink™ PCR Purification Kit (Invitrogen) following the manufacturer's suggested protocol. After purification, a Nanodrop 8000 was used to determine the concentration of DNA. The pCM768 expression vector was isolated from *E. coli* culture using a PureLink™

Quick Plasmid MiniPrep Kit (Invitrogen) following the manufacturer's protocol and the concentration of vector recovered was quantified using a nanodrop 8000.

To create compatible ends for ligation between the PCR fragments and the expression vector pCM768, they were digested with restriction endonucleases (New England BioLabs) indicated in Table 3. The vector RE reaction was 90 µL and contained 8 µg of pCM768, 9 µL of 10x Cutsmart Buffer, 1.5 µL of each RE, and the remaining volume was made up of dH_2O. The RE reaction for the PCR fragment was 60 µL and contained 3 µg of the PCR fragment, 6 µL of 10x Cutsmart Buffer, 1 µL of each RE, and the remaining volume was made up of dH_2O. Both reactions were incubated at 37°C for 3 hrs and were spiked with 1 µL of each RE after 2 hrs. Upon completion of the digest, the PCR fragments were purified using the PureLink™ PCR Purification Kit following the manufacturer's protocol. To obtain pure vector backbone, the digested fragments of pCM768 were separated electrophoretically on a 0.8% agarose gel (1x TAE) stained with 0.3 µg mL^{-1} EtBr and run for 2.5 hrs at 90 V. A HighRanger DNA ladder (Norgen Biotek) was used to compare the fragment sizes and the fragments were then gel extracted using a PureLink™ Quick Gel Extraction Kit (Invitrogen) following the manufacturer's suggested protocol. Upon purification, the pCM768 backbone (vector) and PCR fragments (inserts) were quantified using a nanodrop 8000.

The purified pCM768 backbone was then ligated to the purified and digested PCR fragments (inserts) in 3 reactions using T4 DNA Ligase (New England Biolabs) and molar ratios of 0:1, 3:1, or 6:1 insert:vector. The reaction was incubated at 16°C for 21 hrs in a GeneAmp™ PCR System 9700 thermocycler. The ligated products formed *U. maydis* antisense transcript expression vectors, which were then transformed into Subcloning Efficiency DH5α Competent Cells (Invitrogen) following the manufacturer's suggested

protocol. The plasmid DNA (pDNA) of the antisense transcript expression vectors was isolated from *E. coli* cultures using a PureLink Quick Plasmid MiniPrep Kit following the manufacturer's suggested protocol.

To confirm that the inserts were ligated to the vector, a confirmation digest was performed on the isolated pDNA using the REs indicated in Table 3. The confirmation digest contained 5 µL of pDNA, 1.5 µL of 10x Cutsmart Buffer, 0.5 µL of each RE, and the volume brought up to 15 µL with dH_2O. The reaction was incubated at 37°C for 1.5 hrs and the digested fragments and undigested samples were separated elecrophoretically on a 0.8% agarose gel (1x TAE) that ran at 90V for 1 hr and was visualized with EtBR (0.3 µg mL^{-1}) staining and compared to a HighRanger DNA ladder. The pDNA that produced the expected digestion pattern was then selected for further confirmation through sequencing using Big Dye v3.1 Cycle Sequencing Kit (ThermoFisher Scientific) following the manufacturer's suggested protocol with a modification of the cycles increased to 40x. The reaction products were separated on an ABI 3730 DNA analyzer. The sequences were analyzed, and the quality of reads were assessed using Sequence Scanner Software 2.0 (Applied BioSystems), SeqMan Pro™ 11.2.1 (DNASTAR Inc) was used to trim ends and call bases, and MEGA 7.0.26 was used to confirm sequences by aligning to a reference sequence.

Table 3. Restriction enzymes used to create expression constructs

Plasmid	Restriction Enzymes
521[pCMas-*UMAG_00282*]	*BamH*1 *Hind*III
521[pCMas-*UMAG_01504*]	*BamH*1 *Hind*III
521[pCMas-*UMAG_05213*]	*BamH*1 *Hind*III
521[pCMas-*UMAG_10421*]	*Sph*I *Hind*III

3.8 Preparation of competent protoplasts and *U. maydis* transformation

All *U. maydis* protoplasts were prepared following the protocol outlined in Garcia-Pedrajas *et al*. (2010). Competent 521 protoplasts were transformed with ~1 µg of DNA (antisense expression vector) and ~1 µg of the empty vector pCM768, which was used as a positive control. The transformations were performed following the protocol described in Garcia-Pedrajas *et al*. (2010) with the modification of 100 µL of protoplast mixture used per sample. Genomic DNA was isolated from putative transformants following the organic extraction method outlined in Hoffman and Winston (1987). Successful *U. maydis* transformants were confirmed using PCR with primers designed to amplify the promoter region of the pCM768 vector and the reverse primer used to clone the genomic region corresponding to each antisense (Table 2). Each reaction contained 15.875 µL dH_2O, 2.5 µL 10X DreamTaq Buffer, 2.5 µL 2.5 mM dNTPs, 0.125 µL 5 U μL^{-1} DreamTaq DNA Polymerase, 1 µL 5 µM of each primer and 2 µL 1/10 gDNA. Gene Amp 9700 System (Applied Biosystems) cycling conditions were 95℃ for 10 min, 35 cycles of [95°C for 30

sec, 55°C for 30 sec, 72°C for 1 min], 72°C for 10 min then held at 4°C. PCR products were separated electrophoretically on a 0.8% agarose gel (1X TAE) at 90V for 1 hr and visualized by EtBr (0.3 μg mL^{-1}). Sizes were compared to FullRanger DNA ladder. Successfully transformed strains were cultured and subjected to stresses as outlined above.

CHAPTER FOUR: RESULTS

4.1 Assessing the impact of stress on the growth rate of *U. maydis* haploid strain 521

Cells grown in oxidative (OX) conditions containing different concentrations of H_2O_2 demonstrated altered timelines for cell growth to reach an OD_{600} of 1.0. *U. maydis* haploid cells grown in OX conditions containing 0.0 mM H_2O_2 required ~ 65 hrs, 0.5 mM H_2O_2 required ~ 72 hrs and 1.0 mM and 2.0 mM H_2O_2 required ~ 84 hrs (Figure 2). Wilcoxon Matched Pairs tests indicate that the slower growth rates of 1.0 mM and 2.0 mM H_2O_2 are significantly different compared to the growth rate at 0.0 mM H_2O_2. A concentration of 2.0 mM H_2O_2 was selected for additional stress testing.

Across all four of the single stressed conditions of oxidative (OX), osmotic (OS, minus nitrogen (MN) and minus carbon (MC), growth of *U. maydis* haploid strain 521 was altered compared to the MM control (Figure 3). In the OX condition, growth on solid medium was limited to the concentration of cells spotted at 1.0 OD_{600}. Haploid cells exposed to the OS condition became pigmented and were only able to grow at dilution factors less than 10^{-4}. The cells exposed to the two nutrient conditions did exhibit growth across all the dilution factors; however, the growth was slightly reduced in the MN condition and severely reduced in the MC condition.

When exposed to staggered stressors, exposure to one stress followed by the *U. maydis* haploid strain 521 exhibited altered growth compared to when it was exposed to single stress conditions (Figure 4). When cells were exposed to MN-OX there was limited growth even at 1.0 OD_{600}. This is a further reduction in growth relative to the single stress conditions of MN and OX. Additionally, the cells exposed to MN-OS showed reduced growth relative to the single stress conditions. These cells exhibited a combination of the

phenotypes seen in the single stress conditions. Although the cells exposed to the staggered stress of MN-OS became pigmented, they did not appear as pigmented as those exposed to the OS condition and MN-OS cells grew similarly to those exposed to the MN condition, however slightly reduced.

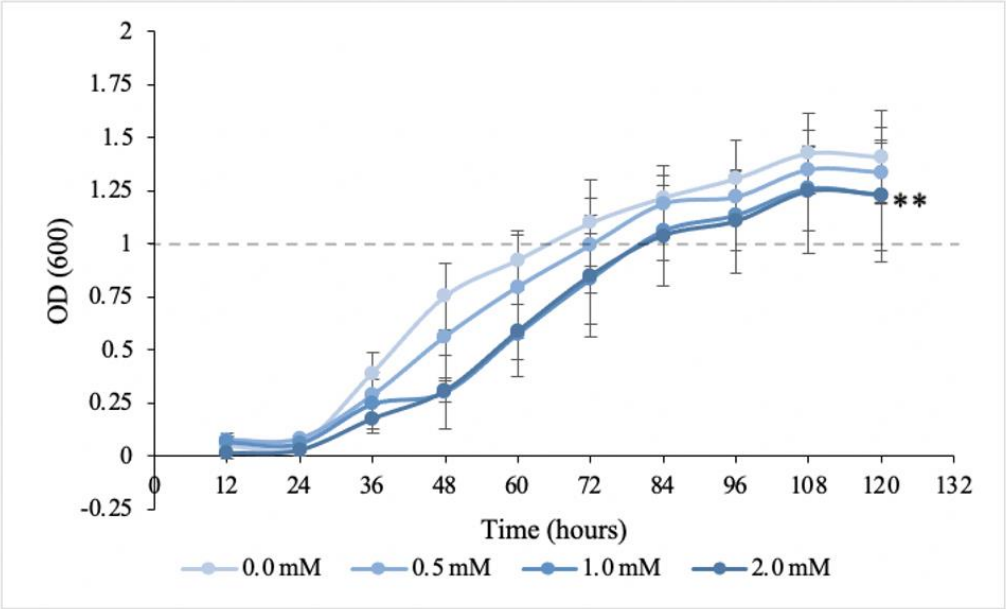

Figure 2. The growth rates of 521 haploid cells grown under oxidative conditions of 1.0 and 2.0 mM H_2O_2 are reduced compared to a 0.0 mM H_2O_2 control. Haploid 521 cells were grown in OX conditions with different concentrations of H_2O_2 at 28^{O}C, 250 rpm for 120 hours. The line colours corresponding to H_2O_2 concentrations are indicated in the legend. The OD_{600} was plotted as an average of three biological replicates with standard deviation reported as error bars. Wilcoxon Matched Pairs test indicated growth curves for 1.0 mM ($p = 0.02142$) and 2.0 mM ($p = 0.01250$) were significantly different compared to 0.0 mM H_2O_2 ($* = p < 0.05$).

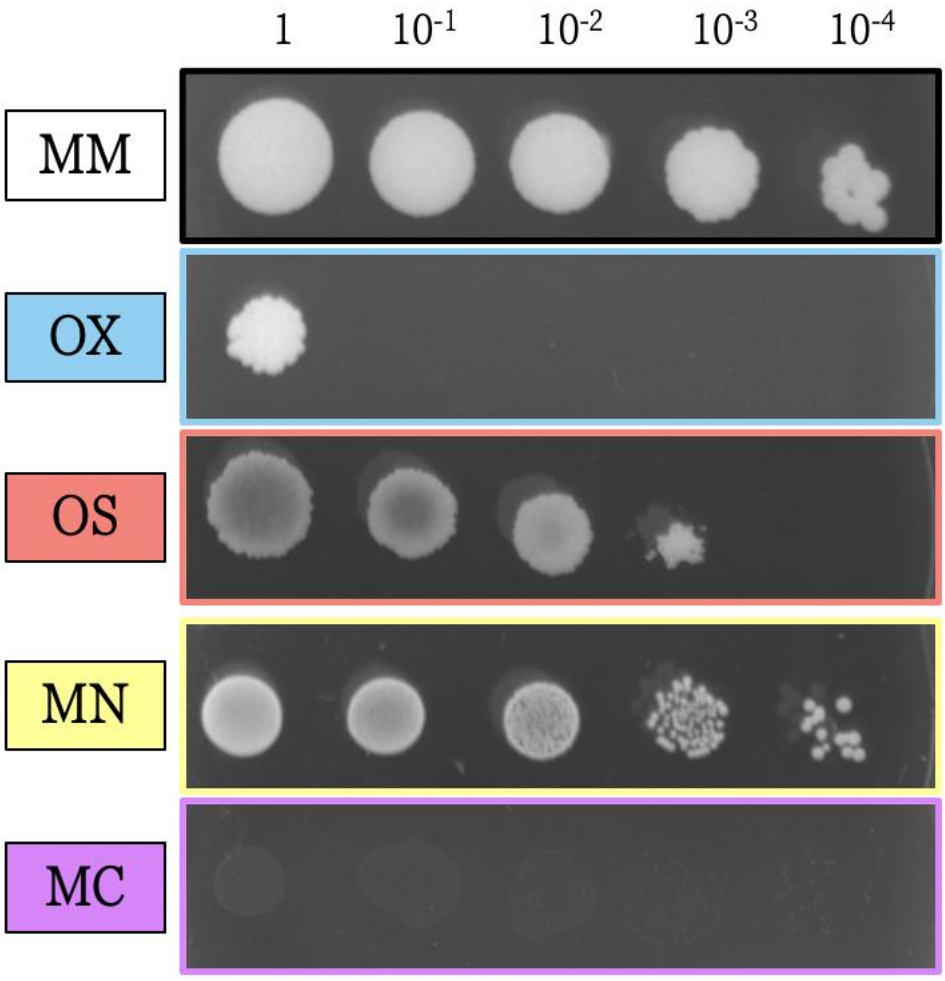

Figure 3. *U. maydis* haploid strain 521 exhibits altered growth in response to single stressors. Cells were normalized to 1.0 OD, serially diluted, and spotted on solid minimal media containing the various stressed conditions, of oxidative (OX), osmotic (OS), minus nitrogen (MN), minus carbon (MC) and the minimal media (MM) control. Plates were incubated at 28^{O}C, and growth was assessed after 5 days. The photographs presented are representative of 5 days of growth.

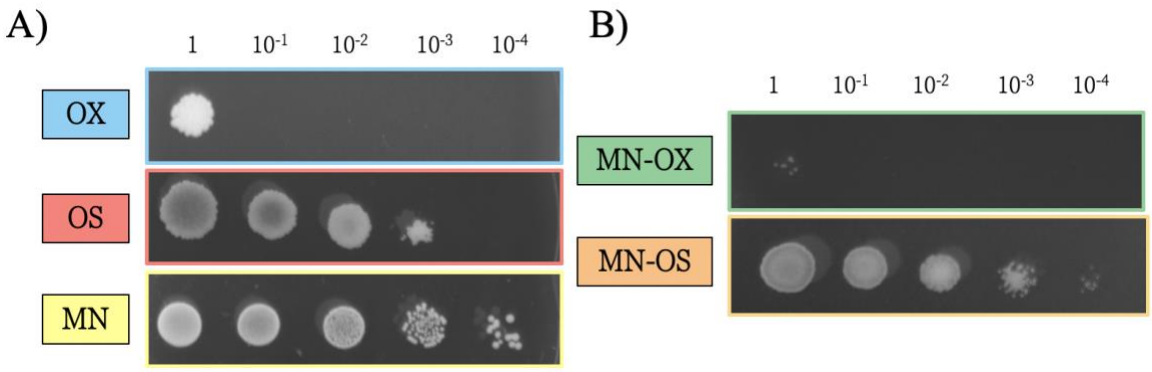

Figure 4. *U. maydis* haploid strain 521 exhibits altered growth in response to staggered stressors. A) Haploid cells were normalized to 1.0 OD, serially diluted, and spotted on solid media containing the various stressed conditions of oxidative (OX), osmotic (OS), and minus nitrogen (MN). B) Haploid cells were grown for 12 hrs in the primary stressed condition of minus nitrogen (MN), washed, normalized to 1.0 OD, serially diluted, and spotted on solid minimal media containing the secondary stressed condition of either oxidative (OX) or osmotic (OS). Plates were incubated at 28^{O}C, and growth was assessed after 5 days. The photographs presented are representative of 5 days of growth.

4.2 Selection of NATs

An objective of this study was the identification of NATs with altered expression levels in response to stressed conditions. The 349 NATs conserved across three related smut fungi identified by Donaldson et al. (2017) were screened by assessing the potential functions of their complementary coding sequences. The predicted functions of these genes were determined based on sequence similarity to previously characterized genes. Based on these similarities the gene/antisense pairs selected were those that corresponded to genes shown

in other systems to be involved in stress response. The gene/antisense pairs were further selected based on the number of NATs present, that is only genes with a maximum of two complementary NATs were selected. This led to the identification of 19 genes and 28 antisense for further analyses. The NATs, their orientation regarding their complementary mRNA, their associated gene descriptions, and previous links to stress are listed in Table 4.

Table 4. NATs complementary to genes with predicted links to stress response

NAT	NAT Orientation	Complementary Gene Description	Previous link to stress
as-*UMAG_00239*	Embedded	related to SSK1 - two-component signal transducer	General, OS (Bahn et al., 2006)
as2-*UMAG_00239*	Embedded		
as-*UMAG_00282*	Embedded	RNA helicase	General (Owttrim, 2006)
as-*UMAG_00592*	Embedded	related to Nuclear receptor co-repressor/HDAC3 complex subunit TBLR1	General (Zhang et al., 2006)
as2-*UMAG_00592*	3` Overlap		
as-*UMAG_00685*	Embedded	probable CBF5 – Centromere Binding Factor / putative rRNA pseuduridine synthase	General (Schwartz et al., 2014)
as-*UMAG_00753*	3` Overlap	related to DDR48 – heat shock protein	OX, OS (*DDR48* | *SGD*, n.d.)
as-*UMAG_00903*	Embedded	related to UBP8 – Ubiquitin-specific protease component of the SAGA complex	General (Yang et al., 2020)
as2-*UMAG_00903*	3` Overlap		
as-*UMAG_00964*	Embedded	related to NOG2 – GTPase involved in ribosomal large subunit-nucleus export	Nutrient, General (Strunk & Karbstein, 2009)
as2-*UMAG_00964*	Embedded		
as-*UMAG_01421*	3` Overlap	related to PHO80 – cyclin	Nutrient (*PHO80* | *SGD*, n.d.)
as-*UMAG_01504*	Embedded	probable Histone H2A	General (*HTA2* | *SGD*, n.d.)
as-*UMAG_01869*	3` Overlap	related to NADH oxidase	

as2-*UMAG_01869*	Embedded		OS (Shi et al., 2016)
as-*UMAG_01891*	Embedded	probable GUF1 – GTP-binding protein	Nutrient (Bauerschmitt et al., 2008)
as-*UMAG_02490*	Embedded	probable FLR1 – Putative H+ antiporter involved in multidrug resistance	OX (Vu & Moye-Rowley, 2018)
as2-*UMAG_02490*	Embedded		
as-*UMAG_03307*	Embedded	related to 5-formyltetrahydrofolate cyclo-ligase	General (*FAU1* | *SGD*, n.d.)
as2-*UMAG_03307*	Embedded		
as-*UMAG_03501*	Embedded	probable DNA topoisomerase II	General (*TOP2* | *SGD*, n.d.)
as-*UMAG_05213*	3` Overlap	related to ADA2 – general transcriptional adaptor or co-activator	General (Chen & Dent, 2021a)
as2-*UMAG_05213*	Embedded		
as-*UMAG_05600*	Embedded	probable UGA2 – succinate semialdehyde dehydrogenase	OX (Coleman et al., 2001)
as2-*UMAG_05600*	Embedded		
as-*UMAG_06063*	Embedded	related to GAD1 – glutamate decarboxylase	General, OX (Coleman et al., 2001)
as-*UMAG_10421*	3` Overlap	related to DPP1 - diacylglycerol pyrophosphate phosphatase	General (Oshiro et al., 2003)
as-*UMAG_10450*	Embedded	related to transcriptional regulator rds2	General (Soontorngun et al., 2012)

4.3 Assessment of NAT expression in response to single stressors

NATs complementary to genes identified as having previous links to stress response were tested to determine if the exposure to stress altered their transcript levels compared to an unstressed control (MM). After *U. maydis* 521 haploid cells were exposed to various stressed conditions (OX, OS, MN, MC), and the MM control for 12 hours, RNA was isolated and transcript levels for each of the 28 identified NATs were assessed using RT-PCR. For each NAT, three cDNA templates were created from RNA isolated from each of the stressed conditions and the control. The reverse transcription reactions were either

primed with oligo$(dT)_{16}$, DEPC-treated H_2O, or strand-specific primers (Table 2). In this screen, oligo$(dT)_{16}$ could prime sense and antisense transcripts as they are both polyadenylated. Since the RT-PCR primers used in this study were designed within the overlapping sense-antisense transcript region, these products could represent a combination of sense and antisense transcripts (Donaldson et al., 2017). Reverse transcriptase reactions were conducted with the absence of an exogenous primer (water) to account for the occurrence of false-priming. This can occur through RNA formation of hairpin structures or through the complementation of endogenous RNAs. Finally, strand-specific primers were designed to specifically target the NATs during RT reactions. The RT-PCR products were used to determine whether NAT transcript levels were altered in any of the stressed conditions compared to the control. A summary of the RT-PCR screens performed on the 28 NATs are shown in Table 5. The RT-PCRs of the five NATs with altered transcript levels in more than one stressed condition are presented in Figure 5.

Of the 28 NATs screened using RT-PCR, only nine had altered levels in at least one stressed condition compared to the control. Of the nine with altered transcript levels in stressed conditions, three had altered levels in only MC, one had altered levels in only MN, three had altered levels in both nutrient conditions (MN, MC), and two had altered levels in all four stressed conditions (Table 5).

The transcript level changes were quantified using RT-qPCR for the five NATs identified as having altered levels in more than one stressed condition during the RT-PCR screen. To ensure false-priming did not impact the quantification, RT reactions were primed using tagged antisense specific primers (Table 2) and a primer complementary to the tagged sequence was used during qPCR. Internal *UMAG_gapdh* transcript levels were

used as a reference to normalize NAT levels in each sample. Relative expression was calculated using the $2^{-\Delta\Delta CT}$ method and samples grown in MM were used as the reference.

Upon exposure to the OX condition, as-*UMAG_00282* had an ~ 1.3-fold upregulation compared to the control and as-*UMAG_5213* had an ~ 1.5-fold upregulation compared to the MM control (Figure 6). However, the other three antisense did not exhibit altered expression in response to this stress condition. When exposed to the OS condition, all five NATs exhibited variation in expression levels across three biological replicates with no overall significant changes compared to the MM control. When exposed to the MN condition, as-*UMAG_00282,* and as-*UMAG_06063* were slightly downregulated compared to the MM control and as-*UMAG_01504* was significantly downregulated compared to the control ($p = 0.04170$). However, as-*UMAG_05213* and as-*UMAG_10421* were, on average, upregulated relative to the MM control. Finally, when exposed to the MC condition, all the NATs except as-*UMAG_06063* were upregulated with as-*UMAG_01504* ($p = 0.03904$) and *UMAG_10421* ($p = 0.01397$) being significantly upregulated relative to the MM control (Figure 6).

Table 5. Summary of the nine NATs with altered expression in RT-PCR screen

NAT	OX	OS	MN	MC
as-*UMAG_00282*	+	+	+	+
as-*UMAG_00592*	-	-	-	+
as2-*UMAG_00903*	-	-	-	+
as-*UMAG_01504*	-	-	+	+
as-*UMAG_01869*	-	-	+	-
as-*UMAG_05213*	-	-	+	+
as-*UMAG_06063*	-	-	+	+
as-*UMAG_10421*	+	+	+	+
as-*UMAG_10450*	-	-	-	+

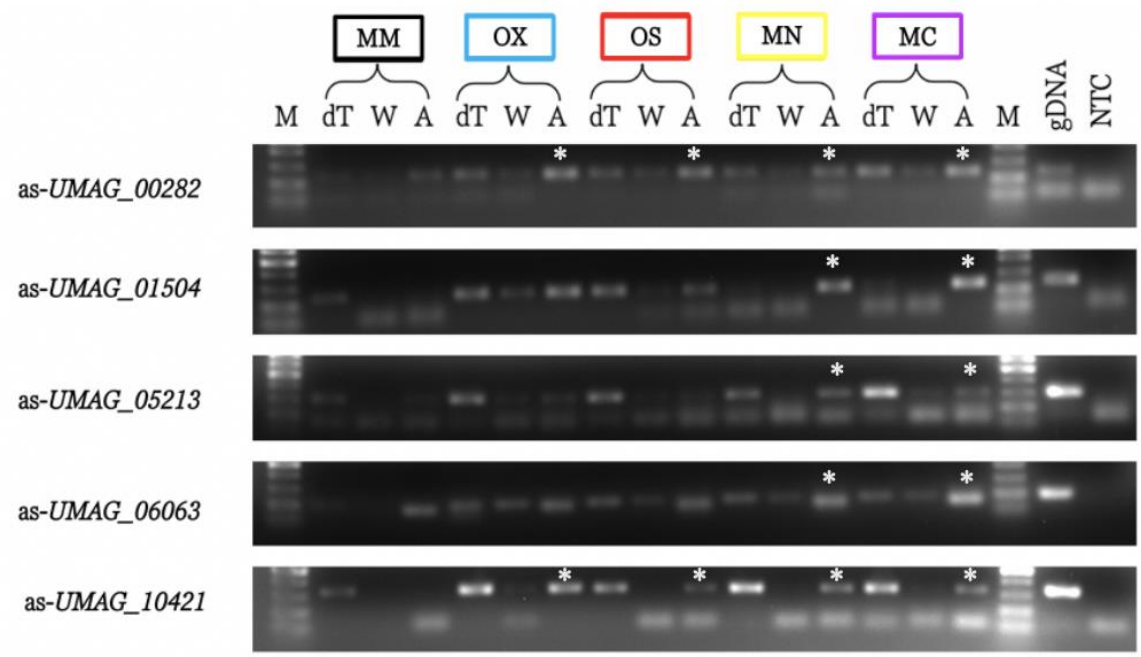

Figure 5. RT-PCR screen identified five NATs with altered transcript levels in multiple stressed conditions compared to the minimal media (MM) control. The origins of the RNA templates were: 521 haploid cells grown in minimal media (MM), 521 haploid cells grown in oxidative conditions (OX), 521 haploid cells grown in osmotic conditions (OS), 521 haploid cells grown in minus nitrogen conditions (MN), or 521 haploid cells grown in minus carbon conditions (MC). The primers used in fist-strand synthesis were oligo$(dT)_{16}$ (dT), DEPC-treated H_2O (W), or antisense specific (A). Genomic DNA (gDNA) and no template (NTC) controls were included for each RT-PCR as well as a size marker (M). Altered antisense transcript levels are indicated (*).

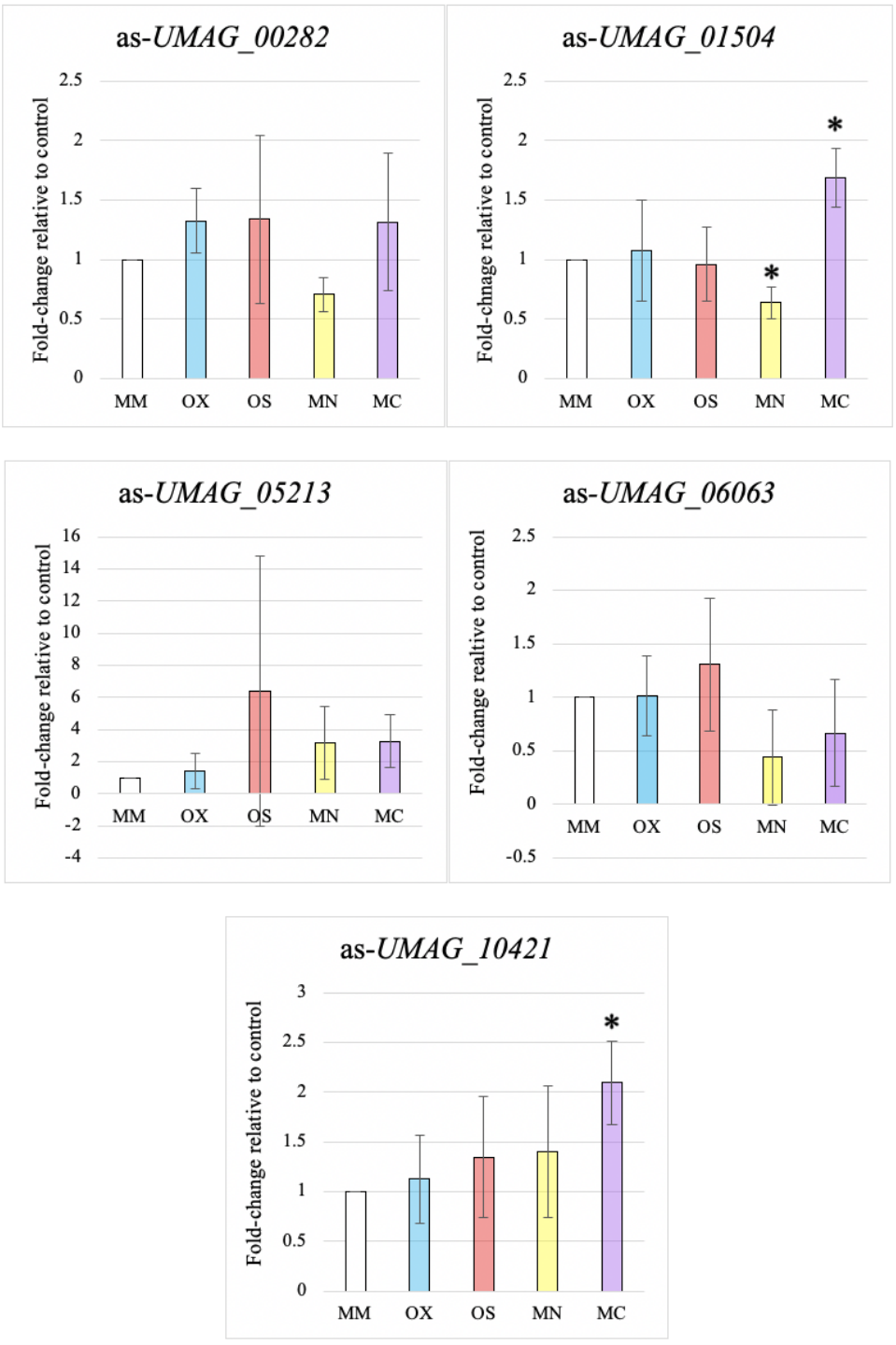

Figure 6. RT-qPCR of NATs supported altered expression in stressed conditions compared to the minimal media (MM) control. RNA was isolated from samples exposed

to stressed conditions for 12 hours. RT-qPCR analysis was performed using three technical replicates for each sample and the housekeeping gene (*UMAG_gapdh)* for normalization. Relative expression was determined using the $2^{-\Delta\Delta Ct}$ method with the samples grown in MM for reference. The average and standard deviation (error bars) of three biological replicates is reported. Statistical differences were calculated comparing each stressed condition back to the MM control using the Student's multiple paired t-test with a Welch correction ($* = p < 0.05$).

4.4 Assessment of NAT expression in response to staggered stressors

Given the altered phenotypes exhibited when *U. maydis* haploid strain 521 was exposed to staggered stressors, RT-qPCR analysis was performed to determine whether these altered phenotypes corresponded to alterations in NAT levels. When haploid cells were exposed to MN-OX conditions, as-*UMAG_00282* and as-*UMAG_01504* exhibited an ~ 2-fold upregulation in expression compared to the control whereas as-*UMAG_05213* and as-*UMAG_10421* did not exhibit altered expression levels (Figure 7). When exposed to MN-OS conditions, as-*UMAG_00282*, as-*UMAG_01504*, and as-*UMAG_10421* exhibited an ~ 1.5-fold upregulation and although there was variation across biological replicates, on average there was a 5-fold upregulating in expression of as-*UMAG_05213*.

When exposed to staggered stressed conditions as-*UMAG_06063* exhibited the greatest change in expression levels. With exposure to MN-OX there was a significant upregulation of ~ 45-fold ($p = 0.00422$) whereas when exposed to MN-OS there was an ~ 20-fold upregulation in NAT expression (Figure 7). This consistent upregulation across

these staggered stressed conditions indicates that the as-*UMAG_06063* may play a role in the response to multiple stress conditions.

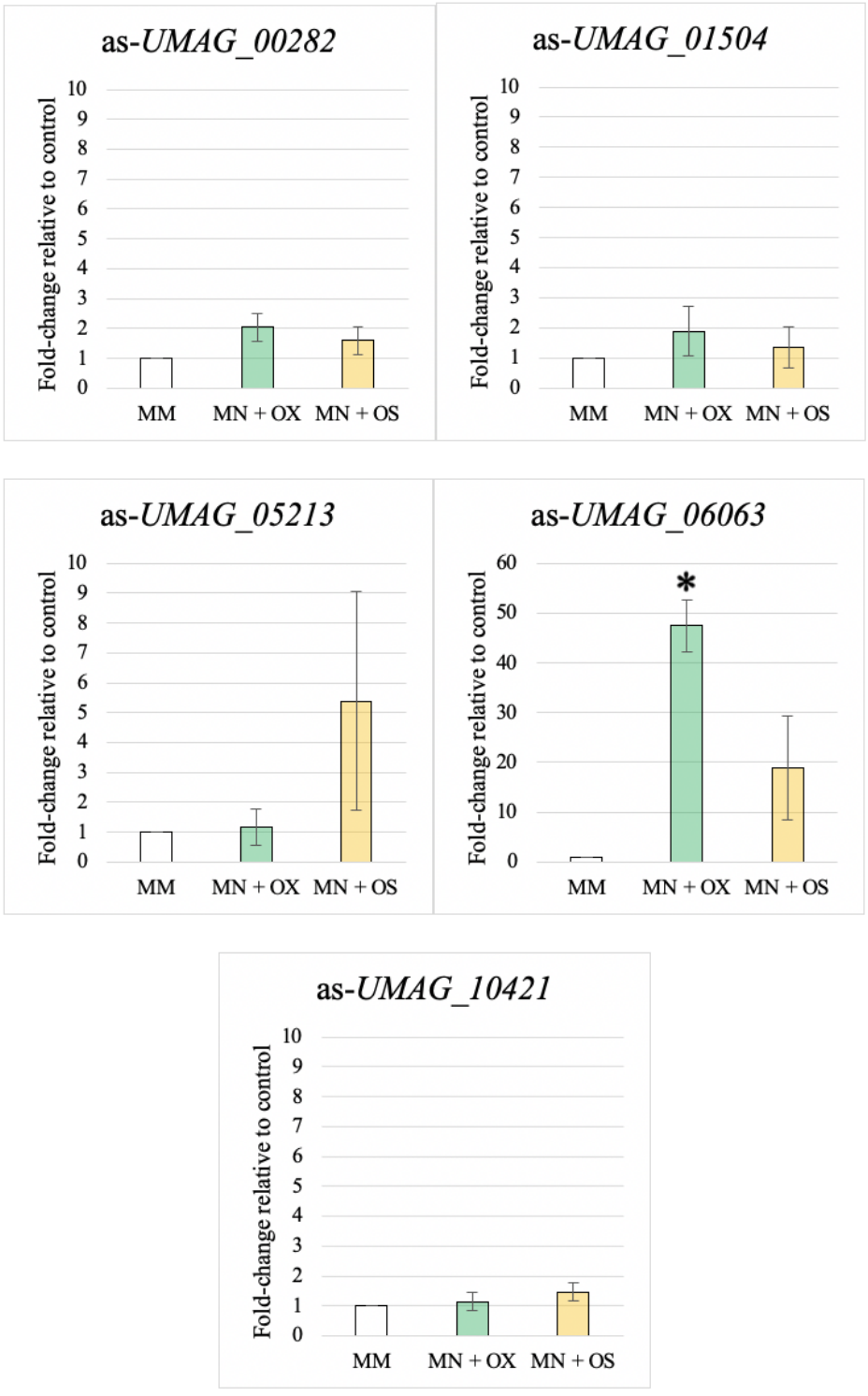

Figure 7. RT-qPCR of NATs indicates altered expression in staggered stressed conditions compared to the minimal media (MM) control. RNA was isolated from samples exposed to MN conditions for 12 hours followed by exposure to either OX or OS conditions for 12 hours. RT-qPCR analysis was performed using three technical replicates for each sample and the housekeeping gene (*UMAG_gapdh)* for normalization. Relative expression was determined using the $2^{-\Delta\Delta Ct}$ method with samples grown in MM used for reference. The average and standard deviation (error bars) of three biological replicates is reported. Statistical differences were calculated comparing each stressed condition back to the MM control using the Student's multiple paired t-test with a Welch correction ($* = p < 0.05$).

4.5 Impact of NAT expression on phenotype

The next focus was to determine whether the expression of NATs would elicit a phenotypic response. To test this, antisense transcript expression vectors were created for four of the identified NATs: as-*UMAG_00282*, as-*UMAG_01504*, as-*UMAG_05213*, and as-*UMAG_10421*. The region of the genome that corresponded to each NAT was inserted into the expression vector pCM768 in a directional manner ensuring the construct expressed the antisense RNA, which was then transformed into *U. maydis* haploid strain 521. Several independent transformants were isolated for each NAT expressing strain as well as for the empty vector strain 521[pCM768]. Successful transformants were confirmed with PCR using a primer designed to amplify the promoter region of pCM768 and a primer used for cloning the antisense (data not shown). Upon confirming the successful transformation of the NAT expressing strains, growth assays were performed to determine whether the

expression of each antisense impacted phenotype. Cells from the 1.0 OD spot on each plate were resuspended and visualized at 400x magnification which revealed no observable changes in cell morphology for the antisense expressing strains compared to the empty vector control (Figure 8).

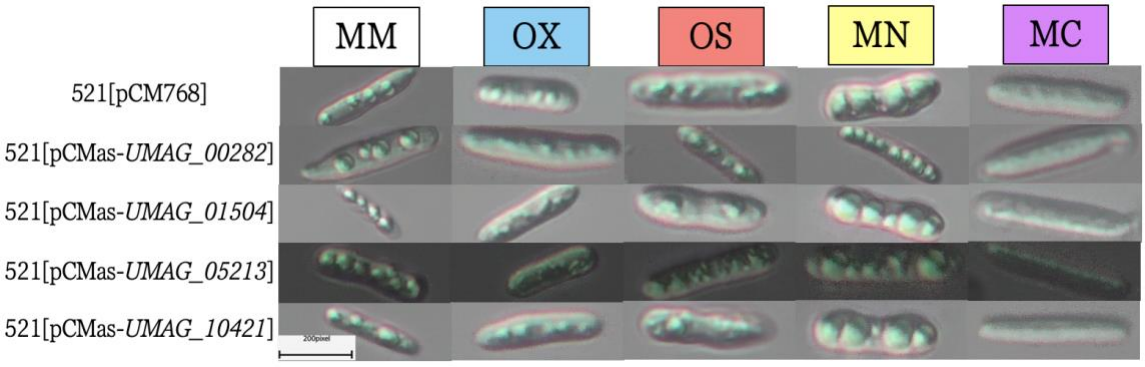

Figure 8. Expression of NATs did not impact the morphology of haploid *U. maydis* cells. Haploid cells spotted on solid minimal media containing the various stressed conditions of either oxidative (OX), osmotic (OS), minus nitrogen (MN), minus carbon (MC) and the minimal media (MM) control were resuspended and visualized with a Zeiss microscope at 400x. Scale bar, 20 μm.

4.5.1 521[pCMas-UMAG_00282*]*

When comparing the growth of three independent transformants of 521[pCMas-*UMAG_00282*] to three independent transformants of 521[pCM768] there was no observable difference in growth across any of the stressed conditions or the control (Figure 9).

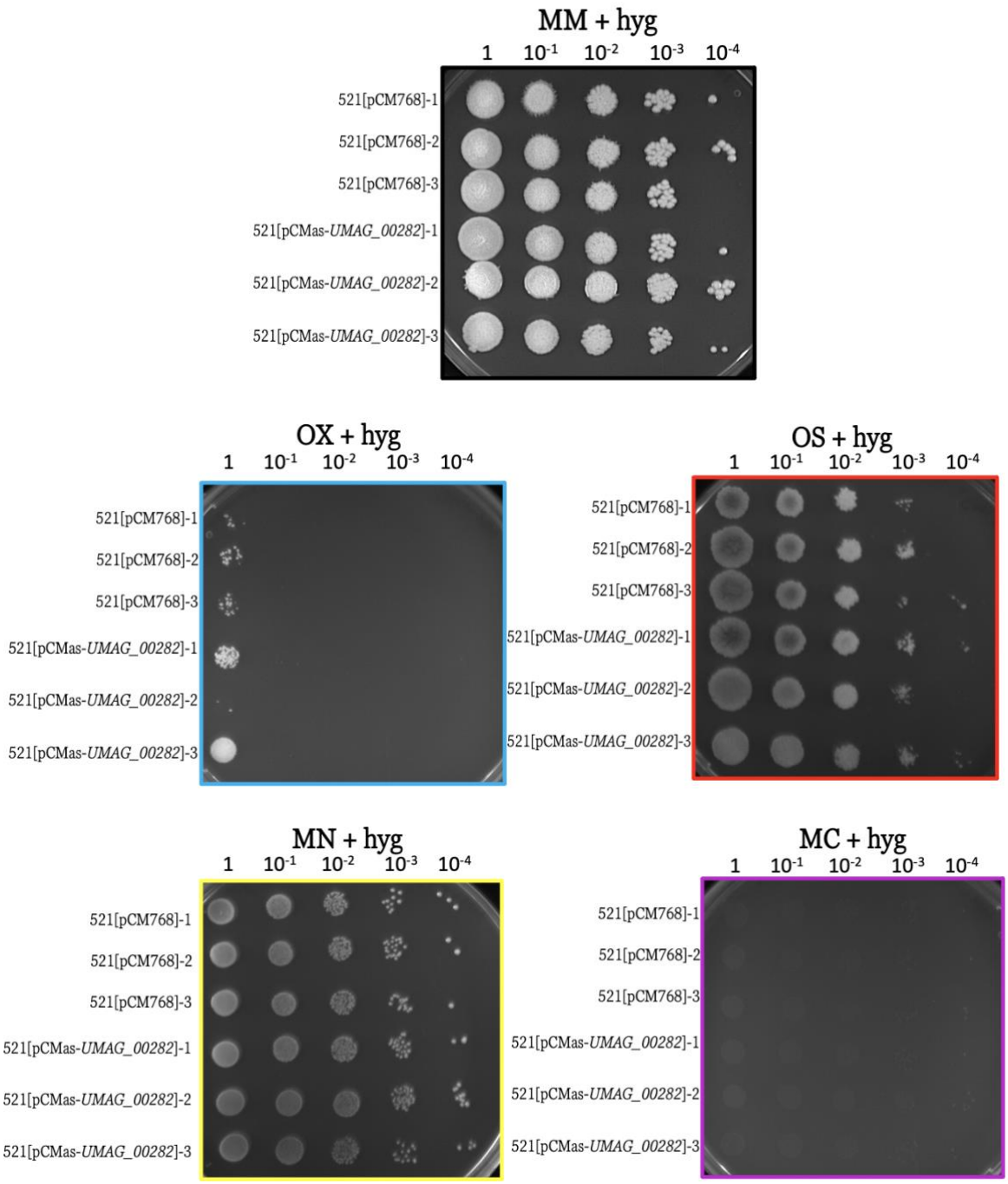

Figure 9. 521[pCMas-*UMAG_00282*] does not exhibit altered growth in response to single stressors. Serially diluted cells of the indicated strains were spotted on solid minimal media containing the various stressed conditions of either oxidative (OX), osmotic (OS), minus nitrogen (MN), minus carbon (MC) and the minimal media (MM) control. Plates

were incubated at 28^{O}C, and growth was assessed after 5 days. The photographs presented are representative of 5 days of growth.

4.5.2 521[pCMas-UMAG_01504*]*

When comparing the growth of three independent transformants of 521[pCMas-*UMAG_01504*] to three independent transformants of 521[pCM768], the stressed conditions that did not elicit a consistent alteration in growth were the OS and MC conditions (Figure 10). In the MM and MN conditions there was an observable reduction in growth of the antisense expressing strains compared to the empty vector controls. In both conditions, the antisense expressing strains exhibited limited growth at the 10^{-3} dilution factor compared to the empty vector controls which sustained growth across all dilutions. In the OX condition the pattern of altered growth in response to stress was flipped. In the empty vector control strains, there was very limited growth observed even at 1.0 OD_{600}. However, in the antisense expressing strains, there was an increase in growth seen across all three of the strains with two of the three independent transformants exhibiting growth at the 10^{-2} dilution factor.

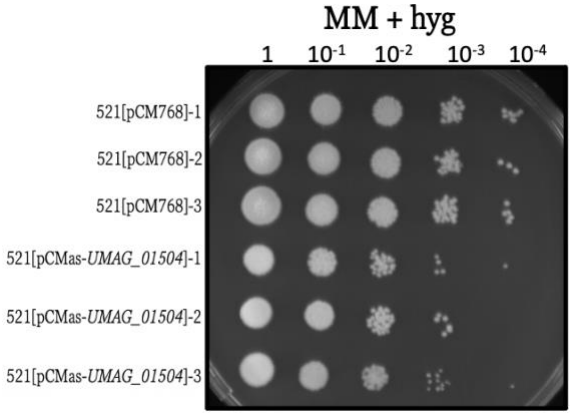

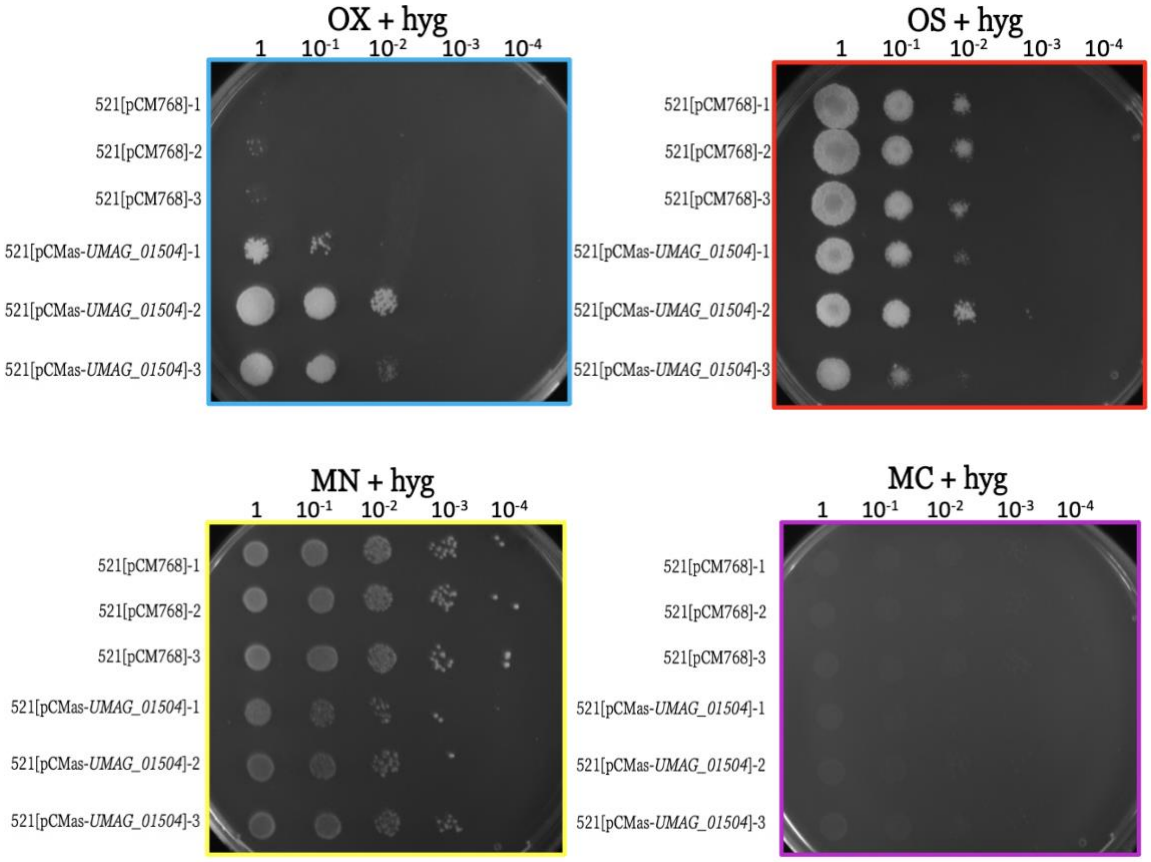

Figure 10. 521[pCMas-*UMAG_01504*] exhibits reduced growth in response to MM and MN conditions and increased growth in response to OX conditions. Serially diluted cells of the indicated strains were spotted on solid minimal media containing the various stressed conditions of either oxidative (OX), osmotic (OS), minus nitrogen (MN), minus carbon (MC) and the minimal media (MM) control. Plates were incubated at 28^{O}C, and growth was assessed after 5 days. The photographs presented are representative of 5 days of growth.

4.5.3 521[pCMas-UMAG_05213*]*

When comparing the growth of three independent transformants of 521[pCMas-*UMAG_05213*] to three independent transformants of 521[pCM768] there was no

observable difference in growth across any of the stressed conditions or the control (Figure 11).

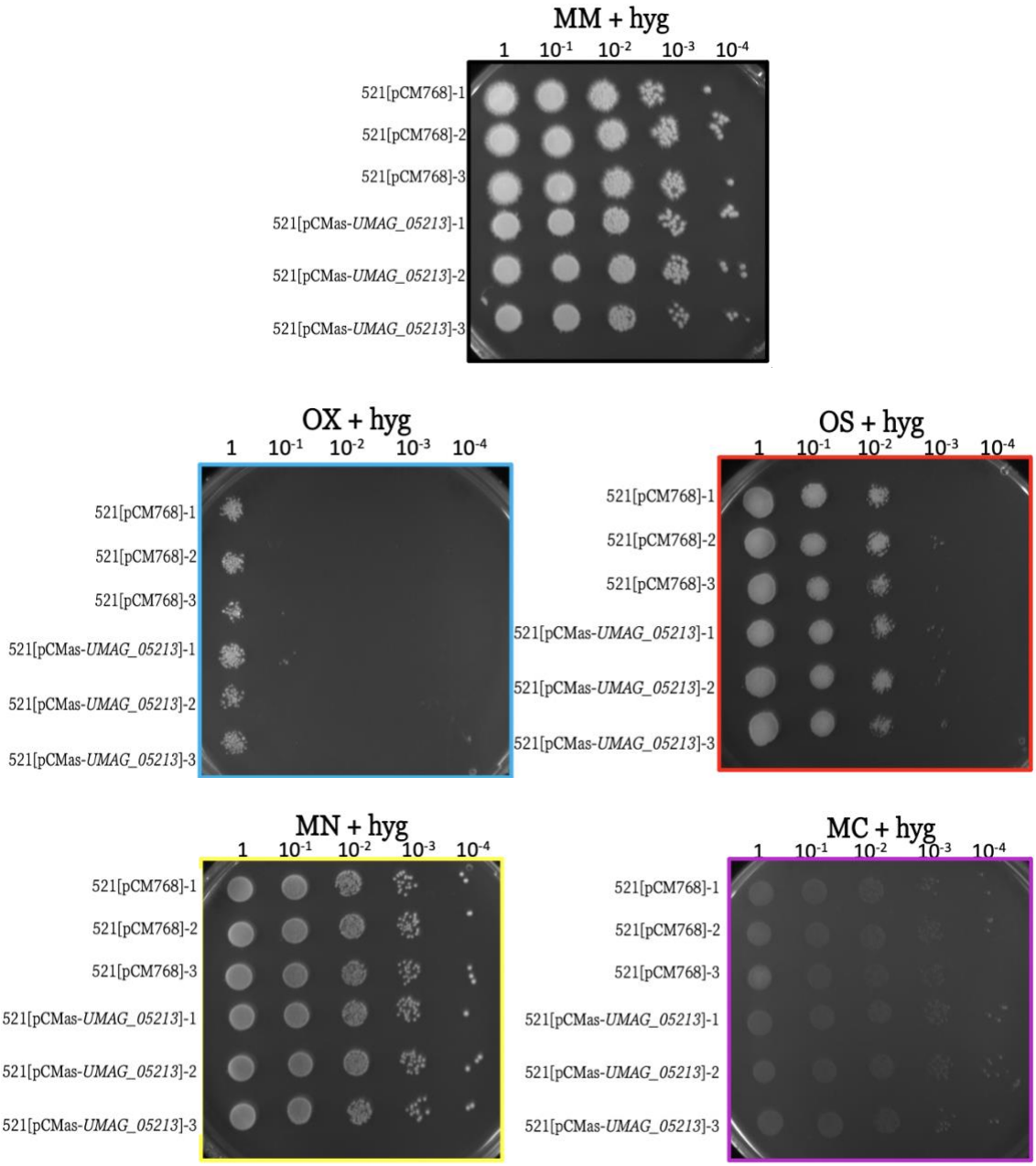

Figure 11. 521[pCMas-*UMAG_05213*] does not exhibit altered growth in response to single stressors. Serially diluted cells of the indicated strains were spotted on solid minimal media containing the various stressed conditions of either oxidative (OX), osmotic (OS),

minus nitrogen (MN), minus carbon (MC) and the minimal media (MM) control. Plates were incubated at 28^{O}C, and growth was assessed after 5 days. The photographs presented are representative of 5 days of growth.

*4.5.4 521[pCMas-*UMAG_10421*]*

When comparing the growth of three independent transformants of 521[pCMas-*UMAG_10421*] to three independent transformants of 521[pCM768] there was no difference in growth observed in the OS, MN, or MC conditions (Figure 12). However, in the MM condition the antisense expressing strains exhibited reduced growth compared to the empty vector controls. In the expressing strains the reduction in growth is seen at the 10^{-3} and 10^{-4} dilutions. Conversely, in the OX condition there was very limited growth observed in the empty vector controls even at 1.0 OD_{600}. However, in the antisense expressing strains there was an increase in growth observed at 1.0 OD_{600} and two of the independent transformants sustained growth at the 10^{-2} dilution factor.

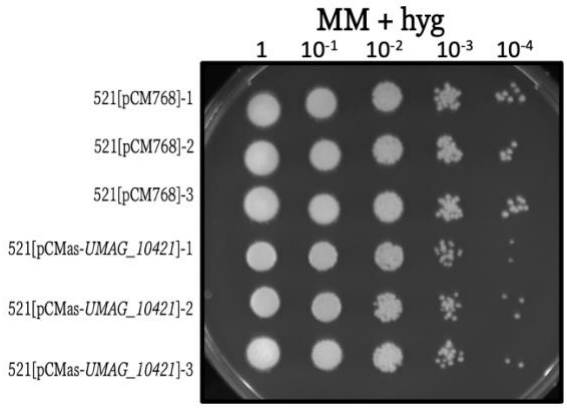

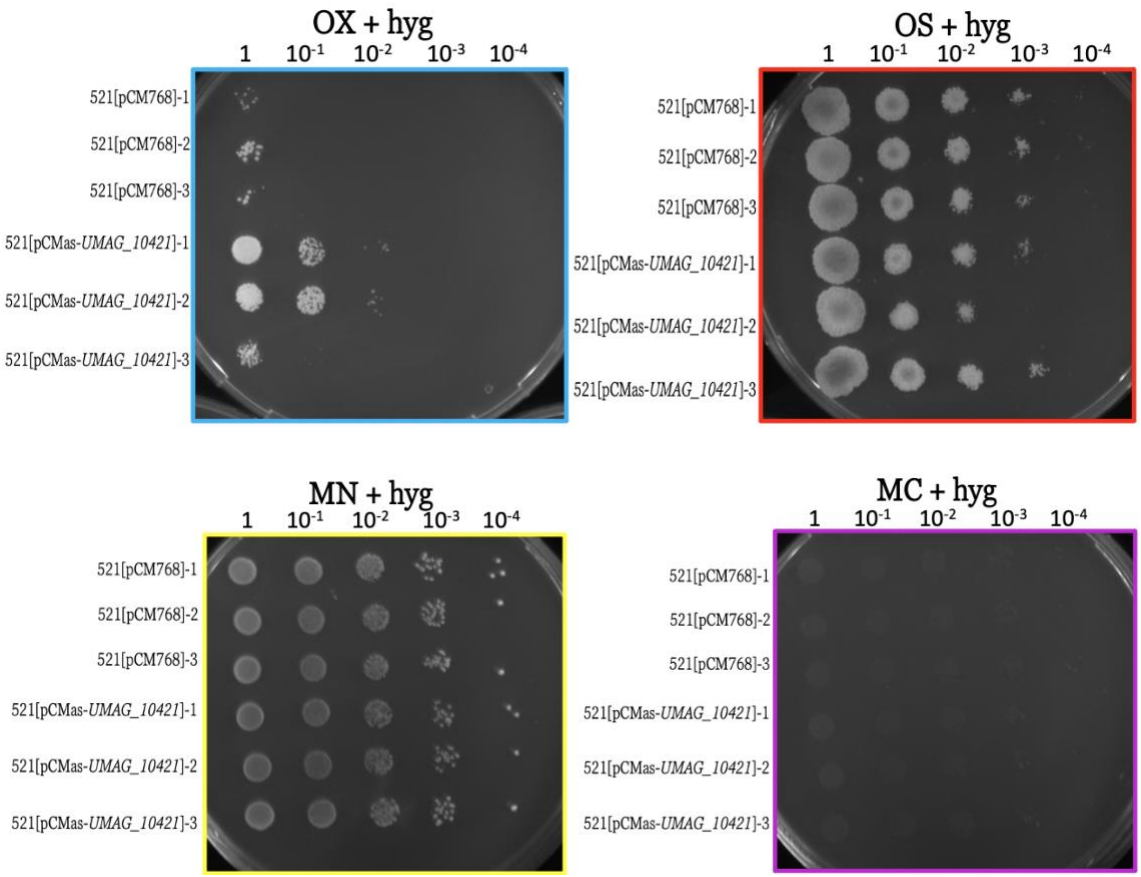

Figure 12. 521[pCMas-*UMAG_10421*] exhibits reduced growth in MM conditions and increased growth in OX conditions. Serially diluted cells of the indicated strains were spotted on solid minimal media containing the various stressed conditions of either oxidative (OX), osmotic (OS), minus nitrogen (MN), minus carbon (MC) and the minimal media (MM) control. Plates were incubated at 28^{O}C, and growth was assessed after 5 days. The photographs presented are representative of 5 days of growth.

4.6 Determining impact of NAT expression on complementary mRNA

Given the altered growth patterns exhibited by the antisense expressing strains 521[pCMas-*UMAG_01504*] and 521[pCMas-*UMAG_10421*] in response to the MM and OX conditions, we wanted to gain an accurate measurement of the altered expression levels for

each of the independent transformants and determine whether this expression impacted the expression of the complementary genes. To gain this understanding, transcript levels were determined through RT-qPCR. Reverse transcriptase reactions were primed using tagged antisense-specific or tagged sense-specific primers to eliminate false-priming. Internal *UMAG_gapdh* transcript levels were used as a reference to normalize NAT levels in each sample. Relative expression was calculated using the $2^{-\Delta\Delta CT}$ method and samples grown in MM were used as the reference.

4.6.1 521[pCMas-UMAG_01504*]*

When the 521[pCMas-*UMAG_01504*] strains were exposed to solid MM we observed a decrease in growth compared to the empty vector controls with the strain denoted as 2 exhibiting no growth at a dilution of 10^{-4}. However, the strains denoted as 1 and 3 still maintained a minimal amount of growth even at the greatest dilution factor (Figure 10). The nature of transforming expression vectors into haploid cells allows for the possibility that different independent transformants can contain different numbers of expression vectors and produce different levels of NATs. To determine the level of NATs present in each of the antisense expressing strains, RT-qPCR analysis was performed. This analysis revealed that when these 521[pCMas-*UMAG_01504*] strains were exposed to MM, NAT expression levels exhibited a 250-fold upregulation in strains 1 and 3 and a 330-fold upregulation in strain 2 relative to the average of three empty vector controls (Figure 13a).

When the 521[pCMas-*UMAG_01504*] strains were exposed to OX conditions on plates, we observed an increase in growth compared to the empty vector controls across all three expressing strains (Figure 10). The smallest increase in growth across these

expressing strains was seen in the strain denoted as 1 as it only exhibited growth until the 10^{-1} dilution factor whereas strains 2 and 3 exhibited growth up until the 10^{-2} dilution factor (Figure 10). When analyzing the RT-qPCR results for NAT expression levels when samples were exposed to OX stress, the pattern of increased expression level of the NAT corresponds to the level of growth seen on solid media. The lowest level of growth was shown in strain 1 which exhibited a 275-fold upregulation in NAT expression, strain 3 exhibited the second highest fold change in NAT levels with a 350-fold upregulation which corresponds to the second greatest increase in growth on solid media. Finally, strain 2 exhibited the greatest increase in growth on OX solid media which corresponds to the highest fold change in NAT expression of 360-fold upregulation relative to the average of three empty vector controls (Figure 13a).

TaqMan qPCR was performed to measure *UMAG_01504* transcript levels in three independent transformants of 521[pCMas-*UMAG_01504*] compared to the average of three empty vector control strains (521[pCM768]). The region of overlap between *UMAG_01504* and as-*UMAG_01504* was amplified and detected using a specific primer/probe combination designed for the *UMAG_01504* transcript (Table 2). While there was some variability in the expression levels of *UMAG_01504* across the three NAT expressing strains exposed to both MM and OX conditions, overall, there was not a significant change in the expression levels of *UMAG_01504* in these conditions compared to the empty vector controls (Figure 13b).

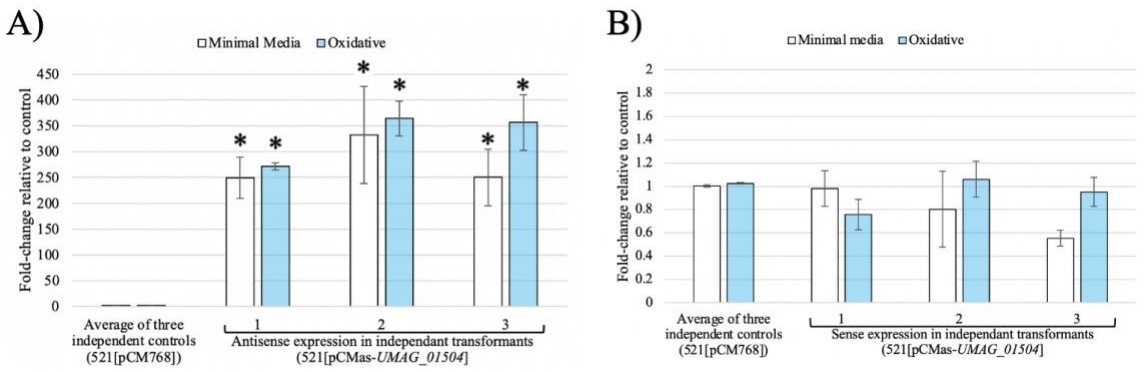

Figure 13. Transformation of pCMas-*UMAG_01504* expression vector into *U. maydis* haploid cells increased NAT levels but did not impact the expression levels of the complementary mRNA. A) Expression of NAT detected in MM and OX conditions B) Expression of mRNA detected in MM and OX conditions. RNA was isolated from samples exposed to MM and OX conditions for 12 hours. Changes in NAT and mRNA expression were determined through TaqMan RT-qPCR analysis. The $2^{-\Delta\Delta Ct}$ method was used to determine NAT expression levels for three independent vector transformed haploid strains (521[pCMas-*UMAG_01504*]) relative to the average of three independently transformed empty vector strains (521[pCM768]). For each sample, the transcript levels of the internal control *UMAG_gapdh* were used as reference. The average and standard deviation (error bars) of three technical replicates for each strain are reported. Statistical differences were calculated comparing each independent transformant of 521[pCMas-*UMAG_01504*] to the average of three independent empty vector transformants (521[pCM768]) using the Student's multiple paired t-test with a Welch correction ($* = p < 0.05$).

4.6.2 521[pCMas-UMAG_10421*]*

When the 521[pCMas-*UMAG_10421*] strains were exposed to solid MM we observed a slight decrease in growth compared to the empty vector controls and the reduction in growth was consistent across the three independent transformants (Figure 12). To determine whether the level of NAT expression was also consistent in this condition across the three strains RT-qPCR analysis was performed. This analysis revealed that when these 521[pCMas-*UMAG_10421*] strains were exposed to MM, NAT expression levels exhibited a range in upregulation from a 100-fold increase seen in strain 3 to a 400-fold increase seen in strain 2 relative to the average of three empty vector controls (Figure 14a).

When the 521[pCMas-*UMAG_10421*] strains were exposed to OX conditions on solid media we saw an increase in growth compared to the empty vector controls across all three expressing strains. The smallest increase in growth across these expressing strains was seen in the strain denoted as 3 as it only exhibited growth at 1.0 OD_{600} whereas strains 1 and 2 exhibited growth up until the 10^{-2} dilution factor (Figure 12). When analyzing the RT-qPCR results for NAT expression levels when samples were exposed to OX stress, the pattern of increased expression level of the NAT corresponds to the level of growth seen on solid media. The lowest level of growth was shown in strain 3 which exhibited a 200-fold upregulation in NAT expression, strain 1 exhibited the second highest fold change in NAT levels with a 390-fold upregulation which corresponds to the second greatest increase in growth on solid media. Finally, strain 2 exhibited the greatest increase in growth on OX solid media which corresponds to the highest fold change in NAT expression of 450-fold upregulation relative to the average of three empty vector controls (Figure 14a).

TaqMan qPCR was performed to measure *UMAG_10421* transcript levels in three independent transformants of 521[pCMas-*UMAG_10421*] compared to the average of three

empty vector control strains (521[pCM768]). The region of overlap between *UMAG_10421* and as-*UMAG_10421* was amplified and detected using a specific primer/probe combination designed for the *UMAG_10421* transcript (Table 2). While there was some variability in the expression levels of *UMAG_10421* across the three NAT expressing strains exposed to both MM and OX conditions, overall, there was not a significant change in the expression levels of *UMAG_10421* in these conditions compared to the empty vector controls (Figure 14b).

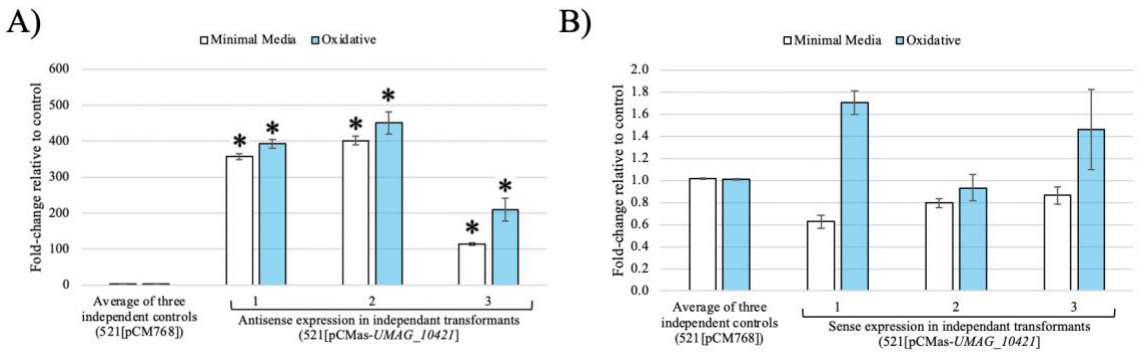

Figure 14. Transformation of pCMas-*UMAG_10421* expression vector into *U. maydis* haploid cells increased NAT levels but did not impact the expression levels of the complementary mRNA. A) Expression of NAT detected in MM and OX conditions B) Expression of mRNA detected in MM and OX conditions RNA was isolated from samples exposed to MM and OX conditions for 12 hours. Changes in NAT and mRNA expression were determined through TaqMan RT-qPCR analysis. The $2^{-\Delta\Delta Ct}$ method was used to determine NAT expression levels for three independent vector transformed haploid strains (521[pCMas-*UMAG_10421*]) relative to the average of three independently transformed empty vector strains (521[pCM768]). For each sample, the transcript levels of the internal control *UMAG_gapdh* were used as reference. The average and standard deviation (error

bars) of three technical replicates for each strain are reported. Statistical differences were calculated comparing each independent transformant of 521[pCMas-*UMAG_10421*] to the average of three independent empty vector transformants (521[pCM768]) using the Student's multiple paired t-test with a Welch correction ($* = p < 0.05$).

CHAPTER FIVE: DISCUSSION

RNA-sequencing and EST analysis of the *U. maydis* genome identified over 4,000 predicted NATs, 2617 of which were considered as having expression detected (Donaldson et al., 2017; Ho et al., 2007). Additionally, this analysis revealed variation in NAT expression across cell-types, which suggests potential roles in modulating gene expression during different developmental stages and environmental conditions (Donaldson & Saville, 2013). A transcriptome comparison of three related smut fungi, *U. maydis, U. hordei,* and *Sporisorium reilianum,* revealed that among the expressed NATs identified in *U. maydis*, 349 are conserved in these smut species (Donaldson et al., 2017). The large proportion of NATs detected in *U. maydis,* the differential expression of NATs across various cell types, and the conservation of NATs amongst these species suggests that they have important functional roles. Previous functional analyses of NATs in *U. maydis* identified their involvement in modulating protein and gene expression, controlling RNA stability, and influencing mitochondrial function and pathogenesis (Donaldson & Saville, 2013; Morrison et al., 2012; Ostrowski & Saville, 2017). This thesis focused on expanding the knowledge surrounding NAT functions in *U. maydis* by investigating a subset of NATs that were complementary to genes with putative connections to stress response. At the beginning of this project, 28 NATs were identified as having potential roles in the stress response of *U. maydis* and through the completion of a series of screens, two NATs have been identified as altering the phenotypic response of *U. maydis* to oxidative stress when over-expressed.

5.1 Assessing the impact of stress on the growth rate of *U. maydis* haploid strain 521

The stress conditions used in this study were selected based on the different environments the fungus could be exposed to in nature. Although many of these stress conditions would be experienced by the *U. maydis* dikaryon or diploid cell, we performed this analysis on the haploid cell as it allowed us to screen a large range of NATs in multiple conditions and gain a preliminary understanding of the relationship between NATs and stress. During the infection of its host, one of the primary plant defences *U. maydis* encounters is an oxidative burst which is caused by the rapid production of ROS at the site of infection (Molina & Kahmann, 2007). Previous studies focused on determining *U. maydis* response to oxidative stress were performed at 0.8 mM and 1.0 mM H_2O_2 (Lanver et al., 2014; Molina & Kahmann, 2007). However, an additional study performed by Nikolaou et al. (2009), revealed that *U. maydis* haploid cells could grow at concentrations of H_2O_2 greater than 1.0 mM. Growth assays were conducted on *U. maydis* haploid strain 521 exposed to various concentrations of H_2O_2 to determine whether the growth exhibited at a higher concentration of H_2O_2 would be sufficient for further analysis such as the isolation of RNA. Although the cells exhibited a reduction in growth rate when exposed to a H_2O_2 concentration of 2 mM, they were still able to reach an OD_{600} of 1.0 which indicates this is a sublethal stress condition and is a viable concentration for further analysis.

Osmotic stress was selected for analysis as it is one of the primary abiotic stressors caused by the changing climate (Hatmi et al., 2018). As extreme weather events including droughts increase in frequency and duration, the alteration in water levels not only impact the interactions plant pathogens have with their hosts but also result in serious constraints on global agriculture and thereby global food security (Hatmi et al., 2018; Wakelin et al., 2018). Salmerón-Santiago et al. (2011), explored the stress response of *U. maydis* and

revealed that there was an approximate 40% reduction in cell growth at 1.0 M NaCl compared to an unstressed control. Additionally, Nikolaou et al. (2009) determined that when *U. maydis* cells were exposed to NaCl concentrations greater than 1.0 M the cells were unable to grow. Growth assays performed on *U. maydis* haploid cells confirmed a reduction in growth at 1.0 M NaCl.

As the climate continues to change, there are alterations in rainfall patterns, temperature, and atmospheric CO_2 concentrations, which impact the nutritional quality of food crops. The increase in CO_2 concentrations have caused a decrease in the concentration of nutrients such as nitrogen and potassium contained in the plant tissues of *Lactuca sativa* and *Spinacia oleracea*. Additionally, drought stress limits the ability for nutrients to be transported throughout the soil which further limits the concentration of nutrients available in plant tissues (Chaudhry & Sidhu, 2022). As the nutrients in plant tissues decrease, this causes a strain on biotrophic plant pathogens which rely on their host plants for nutrient uptake. Additionally, previous studies performed on plant pathogenic fungi have suggested that there may be a connection between nitrogen starvation and fungal colonization of a host plant (Bolton & Thomma, 2008). For example, when the rice blast fungus, *Magnaporthe grisea* was grown in nitrogen-starved conditions *in vitro*, the effector genes associated with host colonization were expressed. Since the same effectors were expressed during colonization and in nitrogen-starved conditions, this suggested that there may be a link between nitrogen stress and virulence such that the pathogen may experience nitrogen limited environments when infecting its host plant (Bolton & Thomma, 2008). During host infection, plant pathogens monitor nitrogen levels to determine their growth rate and changes in morphology. Although these pathogens prefer nitrogen sources such as ammonium and glutamate, most fungi have developed mechanisms to metabolize nitrogen

from both primary and secondary sources (Bolton & Thomma, 2008; Rutherford et al., 2019). Growth assays performed by Ho et al. (2007), demonstrated the ability of *U. maydis* haploid cells to rapidly adapt to nitrogen deprived conditions, which indicates this fungus has likely developed mechanisms to adapt and metabolize all available nitrogen sources for survival and successful infection. The growth assays performed in this study confirm the limited impact a nitrogen starved environment has on the growth of *U. maydis* haploid cells.

Finally, biotrophic plant pathogens must obtain carbon molecules from their host to facilitate growth and successful colonization. Typically, this is done by the release of cell wall degrading enzymes, which facilitate the breakdown of the complex structural polysaccharides that make up the cell wall (Battaglia et al., 2011). This allows for the release of simple sugars that can be metabolized by the fungus and allows for successful infection of the host. The host plant of *U. maydis* is *Z. mays* which is composed of cellulose made of 1,4-β-linked D-glucose units, and hemicellulose polymers which are made of monosaccharide pentose or hexose sugar molecules (Mäkelä et al., 2014). When glucose was removed from the media by Ho et al. (2007), the *U. maydis* cells appeared to stop growing. The growth assays performed in this study indicate that the exposure to a carbon starved environment severely reduces the growth rate of *U. maydis* haploid cells, however, limited growth is sustained.

Although initial assessments were completed using single stressed environments of oxidative (OX), osmotic (OS), nitrogen (MN), and carbon (MC) stress, the environments that fungi inhabit are often complex and dynamic meaning that they likely experience multiple stresses in their lifecycle. To account for these complex environments and to gain a better understanding of the various stress response pathways exhibited by fungi,

additional assessments were completed using a set of staggered stress conditions. Growth assays performed using two staggered stressed conditions of MN followed by either OX or OS exhibited altered growth phenotypes compared to their single stressed counterparts. The combination of MN followed by OX resulted in a reduction in growth exhibited by *U. maydis* haploid cells, whereas cells exposed to MN followed by OS resulted in an increase in growth compared to the single stress of OS. The increased growth exhibited in the MN-OS staggered stress condition indicates the potential use of stress-cross protection mechanisms aiding in the survival of the fungus. The presence of stress-cross protection mechanisms in *U. maydis* could indicate that this model fungus contains a functional core stress response (CSR). Although the CSR for *S. cerevisiae* was hypothesized in the 1990's and confirmed in the early 2000's, the presence of CSRs in other model fungi is still unclear (Brown et al., 2020). The anticipatory stress responses exhibited by *C. albicans* indicate the evolution of a CSR that is specific to the environmental challenges exhibited by its host (Brown et al., 2019, 2020). This suggests that understanding the different environmental stressors that fungi face, the sequence in which they experience these stressors, and how the fungus reacts to these stressors could provide a better understanding and identification of mechanisms involved in the CSRs of model fungal pathogens.

5.2 Identification and analysis of NATs with altered expression levels in response to stressed conditions

At the completion of my undergraduate thesis, 19 genes and 28 associated NATs were identified as having potential roles in the stress response of *U. maydis.* Upon identifying NATs of interest, my graduate work began with RT-PCR screens performed on RNA

isolated from *U. maydis* 521 haploid cells exposed to either OX, OS, MN, MC, or MM conditions. This screen identified nine NATs that had altered expression levels in response to at least one of the single stressed conditions compared to the MM control (Table 5). Based on the RT-PCR results, only NATs that had altered expression levels in more than one stressed condition were selected for additional screening. This limitation was enforced as the alteration of NAT levels in multiple stressed environments suggested a potential role in stress cross-protection. Additionally, quantification of transcript level changes was completed for the five NATs using TaqMan RT-qPCR. Originally this analysis was only completed on the samples isolated from single stressed conditions which revealed that although there were no significant alterations in NAT expression (p-value < 0.05), the NATs did exhibit altered transcript levels relative to the MM control. When RT-qPCR analysis was performed on samples isolated from the staggered stress conditions, significant changes in expression levels were seen in two of the five NATs. Although the RT-qPCR analysis of antisense response to staggered stress demonstrated promising results, this avenue of research was not investigated further in this thesis. Therefore, the NATs selected for the creation of antisense transcript expression vectors were identified based on the response to single stressed environments. The impact of NAT expression on haploid cells exposed to stressed conditions was assessed on solid media. A discussion of the results exhibited for each of the five NATs is presented below.

5.2.1 as-UMAG_00282

The gene complementary to as-*UMAG_00282* was identified through the annotation of the *U. maydis* genome as a putative RNA helicase. Previous studies have

identified RNA helicases as molecular motors which are thought to perform roles in all cellular processes involving RNA metabolism, including the response to biotic and abiotic stress (Owttrim, 2006). Upon completing the initial RT-PCR and RT-qPCR screens for altered expression of NATs in stressed environments, as-*UMAG_00282* was altered in all the stressed conditions compared to the control. The alteration in NAT levels across the various stressed conditions indicated a potential role in a core stress response and if we assume the NAT alters the expression of its complementary mRNA, the broad range of cellular functions that RNA helicases are involved in further supports this idea (Figure 6).

An antisense transcript expressing vector was created for as-*UMAG_00282* and transformed into *U. maydis* 521 haploid cells to create the 521[pCMas-*UMAG_00282*] strain. Growth assays performed on this strain showed that the expression of as-*UMAG_00282* did not impact the growth of *U. maydis* when exposed to the various stressed conditions (Figure 9). Although this antisense did not appear to impact the response to these stress conditions, it is a good candidate for further exploration into other stressed conditions since each helicase in an organism is believed to perform a unique function in cellular physiology (Owttrim, 2006). Additionally, RNA helicases in *S. cerevisiae* have been identified as having altered expression levels when exposed to abiotic stresses including temperature, ethanol and heavy metal stress which further emphasis the need to explore the response to more stress conditions (Owttrim, 2006). Additional studies could focus on alternative RNA helicases as there are an estimated 46 RNA helicases in the *U. maydis* genome, of which 24 have been identified as having associated NATs (Donaldson & Saville, 2013; Seto & Saville, unpublished). Further explorations and investigations into these various RNA helicases and their associated NATs could uncover novel roles in stress response.

5.2.2 as-UMAG_01504

The as-*UMAG_01504* is complementary to a probable histone H2A which was identified through the annotation of the *U. maydis* genome. Investigations into histones found in *U. maydis*, including histone H2A, revealed conserved functions across analogous genes in animals and plants (Anju et al., 2011). In general, histone H2A is a core component of the nucleosome which compacts DNA into chromatin structures thereby modulating access to the DNA template. The role histones play in the formation of chromatin indicates that they have a central role in transcriptional regulation, DNA repair, DNA replication and chromosomal stability (Jeon et al., 2014). The initial RT-PCR and RT-qPCR screens indicated alterations in as-*UMAG_01504* expression levels during the exposure to nutrient stress (Figure 6).

An antisense transcript expressing vector was created for as-*UMAG_01504* and transformed into *U. maydis* 521 haploid cells to create the 521[pCMas-*UMAG_01504*] strain. Growth assays performed on this strain demonstrated altered growth patterns when exposed to MM, OX, and MN conditions compared to the control (Figure 10). Upon identification of the altered phenotypes produced by the 521[pCMas-*UMAG_01504*] strain when exposed to stress, RT-qPCR analysis was performed to determine whether the expression of the NAT impacted its complementary gene. This was done to begin assessing possible mechanism of action of the NAT. Although NAT mechanisms involved in modulating gene expression are still under investigation, three mechanisms of *cis*-acting NATs have been explored in *S. cerevisiae* including transcriptional interference, chromatin remodeling, and double-stranded RNA formation (Donaldson & Saville, 2012; Wight & Werner, 2013). When gene expression is regulated through transcriptional interference,

typically, an increase in NAT transcripts correspond to a decrease in the complementary gene. Similarly, gene regulation through chromatin remodeling results in decreased expression of the complementary mRNA. Finally, gene regulation through double-stranded RNA (dsRNA) formation often results in either increased expression levels of the complementary gene or similar levels of NAT and gene expression (Donaldson & Saville, 2012; Lapidot & Pilpel, 2006). Additionally, functional investigations of NATs in *U. maydis* have revealed roles in altering gene expression through the formation of dsRNA (Donaldson & Saville, 2013; Goulet et al., 2020; Ostrowski & Saville, 2017). Upon analyzing the RT-qPCR results for the NAT and its complementary gene from haploid cells exposed to MM and OX conditions, no significant alteration in gene expression was observed (Figure 13b) even though the NAT had a significant increase in expression (Figure 13a). The lack of altered gene expression of the corresponding mRNA combined with a clear alteration in growth exhibited in the OX condition suggests that this NAT may act through either the production of dsRNA, through influencing a gene located at another loci (*trans*-acting), or through another RNA-mediated manner. Further investigations of this NAT are required to understand its potential role in regulating gene transcription particularly during times of oxidative stress.

5.2.3 as-UMAG_05213

Functional investigations of *UMAG_05213* have yet to be performed in *U. maydis*, however, during the annotation of the genome, it was identified as being related to a transcription coactivator/general transcriptional adapter (*Ada2*) which is a member of the evolutionarily conserved SAGA complex (Chen & Dent, 2021b). In *S. cerevisiae*, Ada2 is

involved in many biological processes. It is a chromatin-binding subunit of the SAGA and SLIK histone acyltransferase complexes, it is involved in histone modification, and it is involved in RNA polymerase II transcription activation. Further investigations into the SAGA complex itself have revealed critical roles in stress response and development in fungi, however, the specific mechanisms of action this complex utilizes are still unclear (Chen & Dent, 2021b). The RT-PCR screen identified as-*UMAG_05213* as having altered expression when exposed to nutrient stress (Figure 5). The RT-qPCR screen confirmed the altered expression in response to nutrient stress and indicated the alteration in expression across the OX and OS stress conditions as well (Figure 6). Additionally, the RT-qPCR screen for the staggered stressors revealed a significant upregulation of this NAT when haploid *U. maydis* cells were exposed to MN-OS staggered stress (Figure 7).

An antisense transcript expressing vector was created for as-*UMAG_05213* and transformed into *U. maydis* 521 haploid cells to create the 521[pCMas-*UMAG_05213*] strain. Growth assays revealed that upon exposure of 521[pCMas-*UMAG_05213*] to MM, OX, OS, MN, and MC conditions, there was no observable alteration in growth (Figure 11). Given the significant alteration in as-*UMAG_05213* expression when exposed to the staggered stress and the variety of biological processes *Ada2* is involved in, the 521[pCMas-*UMAG_05213*] strain is a good candidate for future research focused on the impact of NAT expression on the growth of *U. maydis* when exposed to staggered stress.

5.2.4 as-UMAG_06063

The gene complementary to as-*UMAG_06063* is glutamate decarboxylase (*gad1*) which is an enzyme within the GABA (γ-aminobutyrate)-shunt. Within *S. cerevisiae* the

ortholog to *gad1* and the downstream components of the GABA-shunt are involved in oxidative stress response (Coleman et al., 2001). When analyzed in *U. maydis*, *gad1* was found to be upregulated in times of oxidative stress as well as during appressorium formation. Given the documented role of *UMAG_06063* in oxidative stress, and the fact as-*UMAG_06063* is complementary to an intron-exon junction found within the open reading frame of *UMAG_06063*, it was hypothesized that as-*UMAG_06063* was involved in modulating gene expression through antisense-mediated intron retention. However, RT-PCR and RT-qPCR screens performed on as-*UMAG_06063* indicated no alteration in NAT expression when *U. maydis* haploid cells were exposed to OX conditions. Although there was no significant alteration in NAT expression during the exposure to single stress conditions, RT-qPCR analysis of *U. maydis* exposure to staggered stress conditions indicated a significant upregulation of as-*UMAG_06063*. This alteration of NAT expression upon exposure to staggered stressors indicates that this gene may play a role in a stress cross-protection. Additionally, the upregulation of *gad1* in *U. maydis* during appressorium formation and oxidative stress indicate a potential role in protecting the fungus against plant defences since the formation of appressorium coincides with the oxidative burst exhibited by the host plant's defence system (Lanver et al., 2014). If this gene did contribute to the protection of the fungus during plant infection it would also influence the virulence of the pathogen. Although the deletion of *gad1* in *U. maydis* did not impact the survival of cells in oxidative stress or impact the virulence of *U. maydis*, this could be due to the redundancy found within the *U. maydis* genome as three glutamate decarboxylases have been identified (Lanver et al., 2014). The documented roles of *gad1* in stress response combined with the consistent upregulation of as-*UMAG_06063* across

the staggered stress conditions makes this NAT a good candidate for future functional investigation as it relates to stress-cross protection.

5.2.5 as-UMAG_10421

The gene complementary to as-*UMAG_10421* was identified through the *U. maydis* genome annotation as being related to *DPP1* which encodes a diacylglycerol pyrophosphate phosphatase. Investigations into *DPP1* have been performed in *S. cerevisiae* and revealed roles in phospholipid metabolism and as a lipid signal molecule during stressed conditions (Oshiro et al., 2003). Deletion of *DPP1* in *S. cerevisiae* showed that this gene is not essential for cell growth and the deletion strain demonstrated no alteration in growth or cell morphology compared to wild type (Toke et al., 1998). Initial RT-PCR and RT-qPCR screens identified as-*UMAG_10421* as having altered expression levels across all tested stress conditions with the greatest alteration occurring when exposed to MC conditions (Figure 6). Investigations into the regulation of *DPP1* in *S. cerevisiae* revealed that when cells were exposed to nutrient starvation conditions, causing cells to cease proliferation, *DPP1* expression was induced (Oshiro et al., 2003; Werner-Washburne et al., 1993). Given the limited growth exhibited when *U. maydis* haploid cells were exposed to MC conditions it was thought that the altered expression levels demonstrated by as-*UMAG_10421* could indicate a role in regulating the expression of its complementary gene.

An antisense transcript expressing vector was created for as-*UMAG_10421* and transformed into *U. maydis* 521 haploid cells to create the 521[pCMas-*UMAG_10421*] strain. Growth assays revealed that upon exposure of 521[pCMas-*UMAG_10421*] to OS,

MN, and MC conditions, there was no observable alteration in growth (Figure 12). However, when exposed to MM conditions 521[pCMas-*UMAG_10421*] demonstrated a slight decrease in growth and when exposed to OX conditions, 521[pCMas-*UMAG_10421*] demonstrated an increase in growth compared to the control (Figure 12). RT-qPCR analysis was performed to determine whether the altered phenotypes exhibited by the 521[pCM-as-*UMAG_10421*] strain in MM and OX conditions corresponded to altered expression levels of the complementary gene. Although no significant alterations in expression levels were detected for the complementary gene (Figure 14b) when NAT expression was significantly upregulated (Figure 14a), the clear alteration in growth exhibited by the 521[pCM-as-*UMAG_10421*] strain in OX conditions indicates that this NAT may play a role in modulating the response to OX stress. Overall, further investigations of this NAT are required to understand its potential role in regulating gene transcription and protein expression during times of oxidative stress.

Although the expression lines created for these antisense demonstrate a potential role in NAT mediated responses to stress, they do have several limitations. First, due to the nature of transforming expression vectors into haploid cells there is the potential for independent transformants to contain different numbers of expression vectors. The variation in expression vectors present in these independent transformants could explain the variation in growth exhibited across the expressing strains exposed to the OX condition (Figure 12). RT-qPCR analysis revealed altered levels of antisense expression across the independent transformants of 521[pCM-as-*UMAG_10421*] (Figure 14a) which could indicate the presence of a different number of expression vectors. Additionally, the independent transformants of 521[pCM-as-*UMAG_10421*] that demonstrated the greatest amount of growth in OX conditions also exhibited the highest fold change difference

compared to the empty vector control. This suggests that *U. maydis* haploid cells may better survive OX conditions when higher levels of this antisense transcript are expressed. Another limitation of using the pCM768 expression vector to express these NATs is that these constructs are expressing the NATs in *trans* rather than in *cis*. Given the potential roles NATs can have in regulating gene expression through transcriptional interference, the expression of NATs in *trans* may limit the information gained through this analysis. Additionally, these vectors are autonomously replicating and thereby continuously express the NATs. The continuous expression of these NATs could negatively impact the growth of *U. maydis* haploid cells in unstressed conditions. In both the 521[pCM-as-*UMAG_01504*] and 521[pCM-as-*UMAG_10421*] strains the growth was increased when exposed to the OX condition however it was reduced in the MM condition (Figure 10, 12). This suggests that in times of OX stress the expression of these NATs is beneficial, however when these NATs are expressed in unstressed conditions it could be harmful.

Although there is still a lot of research to be done regarding identifying and describing the roles NATs have in modulating the stress response of *U. maydis*, this research demonstrates the merit in exploring the connection between NATs and stress in fungi. Upon the completion of this thesis, I was able to narrow down the initial 28 identified NATs with potential roles in stress response to two NATs that, when expressed, alter the growth patterns of *U. maydis* haploid cells when exposed to MM and OX conditions. Additionally, the analysis of NAT expression in response to staggered stress conditions identified two other NATs with potential roles in stress-cross protection. Although previous research on the stress responses of fungi has focused on functionally characterizing protein-coding genes involved in these pathways, this research indicates that the functional characterization of NATs may be equally important in gaining a comprehensive

understanding of these stress response pathways. After all, ncRNAs are no longer simply considered 'junk' DNA and NATs are not just 'transcriptional noise' (Donaldson & Saville, 2012; Liu et al., 2021; Pelechano & Steinmetz, 2013). Their roles in modulating gene expression and other biological process are becoming increasingly well documented and this research is merely the tip of the iceberg in terms of exploring their roles in the stress responses of pathogenic fungi.

5.3 Future directions

Future experiments should begin with quantification of the altered growth exhibited by the antisense expressing strains by performing liquid growth assays. Additionally, these antisense expressing strains should be exposed to staggered stressors to determine whether they exhibit any altered phenotypes. The antisense expressing strains 521[pCMas-*UMAG_01504*] and 521[pCM-as-*UMAG_10421*] should undergo S1 nuclease digestion to determine whether dsRNA formation is occurring when we observe the altered phenotypes. Given the altered expression levels demonstrated by the as-*UMAG_06063* in response to staggered stress conditions, an antisense expression vector should be created for this NAT and be transformed into *U. maydis* haploid cells. From there, this strain should be exposed to staggered stress environments to determine whether the expression of the NAT impacts the survival and growth of the fungus. Additionally, future experiments could focus on the current lack of knowledge surrounding the function of the genes complementary to the five NATs of interest in *U. maydis*. The creation of deletion and expression strains for the genes complementary to these NATs could aid in identifying the roles in stress response for both

the gene and its complementary NAT. These strains would also function as controls for future analysis in determining the impact of NAT expression on phenotype.

Research on NAT mediated roles in stress response could focus on the interaction the fungus has with its host, particularly at the time of initial infection when host defences start to rise. By exposing these antisense expressing strains and wild type to a sequence of stressed environments that mimic stressors caused by the host, we could gain an understanding of potential stress-cross protection pathways, and thereby determine whether these NATs play a role in the pathogenesis of the fungus. Additionally, the impact NAT expression has on the interactions with the host plant could be determined through the creation of strains that constitutively express the NATs and are integrated into the *U. maydis* genome at the *ip* locus. These strains could then be analyzed using seedling pathogenesis assays thereby allowing us to investigate the role these NATs play in protecting the fungus against host defences. The addition of the staggered stressors was the first step in analyzing the roles these NATs play in natural environments, the incorporation of simultaneous stressors could further elucidate the potential roles these NATs play in modulating the stress response of the fungus. Finally, alternative NATs could also be selected to determine their role in the stress response of the fungus. When the NATs of interest were originally selected, we eliminated several genes that had documented roles in stress response due to the large number of associated NATs. Future research could focus on exploring those genes and screening their associated NATs for potential roles in modulating gene expression when exposed to stress.

CHAPTER SIX: CONCLUSION

The research presented in this thesis was designed to expand the knowledge surrounding the function of NATs by identifying potential roles in modulating the stress response of the model fungus, *U. maydis*. This investigation started with 28 NATs identified as having potential roles in stress responses. After selecting four stress conditions (OX, OS, MN, MC) and completing a series of RT-PCR and RT-qPCR screens, I was able to successfully identify five NATs that had altered expression levels in multiple stress conditions compared to the MM control. The alteration of NAT expression in these stressed conditions suggested that they may have roles in modulating the fungus's response to stress. Additionally, *U. maydis* haploid cells were exposed to two staggered stress conditions of MN-OX and MN-OS to explore potential roles in stress-cross protection. The alteration in growth of the haploid *U. maydis* cells when exposed to these staggered stressed conditions combined with the significant alteration in the expression levels of two NATs in cells exposed to these conditions indicates potential roles in stress-cross protection. However, additional research is needed to confirm and expand upon these findings. To further explore the potential role of the five identified NATs, antisense expressing strains were created for four of the NATs. Upon exposing these antisense expressing strains to stressed environments, two were identified as exhibiting altered growth patterns in MM and OX conditions compared to empty vector controls. Given the clear alteration in phenotype exhibited by these antisense expressing strains, RT-qPCR analysis was performed to evaluate whether the altered NAT expression impacted the expression of the genes complementary to these NATs. That analysis revealed although NAT expression was significantly upregulated compared to empty vector controls, there was not a significant

alteration in the expression levels of their complementary genes. This suggests that these NATs may be involved in modulating gene expression through the formation of dsRNA or that they may be acting in *trans* rather than in *cis*. However, further analysis is required before any definitive statements can be made regarding their modes of action and their roles in modulating the stress response of *U. maydis*.

Further research is required to better understand both the mechanisms of action these NATs exhibit and their roles in stress response. This research has laid the groundwork for future investigations into the connections between NATs and stress responses in pathogenic fungi. By identifying RNA-mediated responses to stress, we can start to form a better understanding of how organisms adapt to and survive changing climactic conditions. Ultimately, through developing a better understanding of the mechanisms that pathogens use to survive stress conditions, whether induced through their host's defences or through the changing climate, we hope to provide novel targets to combat the increasing prevalence and severity of fungal diseases and limit their impact on the global food supply, thereby contributing to a decrease in global hunger.

REFERENCES

Anderson, P. K., Cunningham, A. A., Patel, N. G., Morales, F. J., Epstein, P. R., & Daszak, P. (2004). Emerging infectious diseases of plants: pathogen pollution, climate change and agrotechnology drivers. *Trends in Ecology & Evolution*, *19*(10), 535–544. https://doi.org/10.1016/J.TREE.2004.07.021

Anderson, R., Bayer, P. E., & Edwards, D. (2020). Climate change and the need for agricultural adaptation. *Current Opinion in Plant Biology*, *56*, 197–202. https://doi.org/10.1016/J.PBI.2019.12.006

Anju, V., Kapros, T., & Waterborg, J. H. (2011). Identification of a replication-independent replacement histone H3 in the basidiomycete Ustilago maydis. *Journal of Biological Chemistry*, *286*(29), 25790–25800. https://doi.org/10.1074/jbc.M111.254383

Bahn, Y. S., Kojima, K., Cox, G. M., & Heitman, J. (2006). A Unique Fungal Two-Component System Regulates Stress Responses, Drug Sensitivity, Sexual Development, and Virulence of Cryptococcus neoformans. *Molecular Biology of the Cell*, *17*(7), 3122. https://doi.org/10.1091/MBC.E06-02-0113

Battaglia, E., Benoit, I., van den Brink, J., Wiebenga, A., Coutinho, P. M., Henrissat, B., & de Vries, R. P. (2011). Carbohydrate-active enzymes from the zygomycete fungus Rhizopus oryzae: A highly specialized approach to carbohydrate degradation depicted at genome level. *BMC Genomics*, *12*(1), 1–12. https://doi.org/10.1186/1471-2164-12-38/FIGURES/2

Bauerschmitt, H., Funes, S., & Herrmann, J. M. (2008). The membrane-bound GTPase Guf1 promotes mitochondrial protein synthesis under suboptimal conditions. *Journal of Biological Chemistry*, *283*(25), 17139–17146. https://doi.org/10.1074/jbc.M710037200

Bolton, M. D., & Thomma, B. P. H. J. (2008). The complexity of nitrogen metabolism and nitrogen-regulated gene expression in plant pathogenic fungi. *Physiological and Molecular Plant Pathology*, *72*(4–6), 104–110. https://doi.org/10.1016/J.PMPP.2008.07.001

Bonghan Berinyuy, E., Ngo Ngo, V., Fokunang, C., Annih Grace, M., Estella Achick, T.-F., Eustace Bonghan, B., Evelyn Bih, M., Valery Ngo, N., James Ajeck, M., Tangham Bobyiga Prudence, G., Charles Ntungwen, F., & Charles Ntungwen An Overview, F. (2019). Overview of the impact of climate change on pathogens, pest of crops on sustainable food biosecurity. *International Journal of Ecotoxicology and Ecobiology*, *4*(4), 114–124. https://doi.org/10.11648/j.ijee.20190404.15

Brown, A. J. P., Cowen, L. E., di Pietro, A., & Quinn, J. (2017). Stress Adaptation. *Microbiology Spectrum*, *5*(4). https://doi.org/10.1128/microbiolspec.funk-0048-2016

Brown, A. J. P., Gow, N. A. R., Warris, A., & Brown, G. D. (2019). Memory in Fungal Pathogens Promotes Immune Evasion, Colonisation, and Infection. *Trends in Microbiology*, *27*(3), 219–230. https://doi.org/10.1016/J.TIM.2018.11.001

Brown, A. J. P., Larcombe, D. E., & Pradhan, A. (2020). Thoughts on the evolution of Core Environmental Responses in yeasts. *Fungal Biology*, *124*(5), 475. https://doi.org/10.1016/J.FUNBIO.2020.01.003

Causton, H. C., Ren, B., Sang Seok Koh, Harbison, C. T., Kanin, E., Jennings, E. G., Tong Ihn Lee, True, H. L., Lander, E. S., & Young, R. A. (2001). Remodeling of

yeast genome expression in response to environmental changes. *Molecular Biology of the Cell*, *12*(2), 323–337. https://doi.org/10.1091/mbc.12.2.323

Chaudhry, S., & Sidhu, G. P. S. (2022). Climate change regulated abiotic stress mechanisms in plants: a comprehensive review. *Plant Cell Reports*, *41*(1), 1–31. https://doi.org/10.1007/S00299-021-02759-5/TABLES/3

Chen, Y. J. C., & Dent, S. Y. R. (2021a). Conservation and diversity of the eukaryotic SAGA coactivator complex across kingdoms. *Epigenetics & Chromatin 2021 14:1*, *14*(1), 1–11. https://doi.org/10.1186/S13072-021-00402-X

Chen, Y. J. C., & Dent, S. Y. R. (2021b). Conservation and diversity of the eukaryotic SAGA coactivator complex across kingdoms. *Epigenetics & Chromatin 2021 14:1*, *14*(1), 1–11. https://doi.org/10.1186/S13072-021-00402-X

Coleman, S. T., Fang, T. K., Rovinsky, S. A., Turano, F. J., & Moye-Rowley, W. S. (2001). Expression of a glutamate decarboxylase homologue is required for normal oxidative stress tolerance in Saccharomyces cerevisiae. *Journal of Biological Chemistry*, *276*(1), 244–250. https://doi.org/10.1074/jbc.M007103200

Corredor-Moreno, P., & Saunders, D. G. O. (2020). Expecting the unexpected: factors influencing the emergence of fungal and oomycete plant pathogens. *New Phytologist*, *225*(1), 118–125. https://doi.org/10.1111/NPH.16007

DDR48 | SGD. (n.d.). Retrieved April 22, 2020, from https://www.yeastgenome.org/locus/S000004784

de Vallavieille-Pope, C., Bahri, B., Leconte, M., Zurfluh, O., Belaid, Y., Maghrebi, E., Huard, F., Huber, L., Launay, M., & Bancal, M. O. (2018). Thermal generalist behaviour of invasive Puccinia striiformis f. sp. tritici strains under current and future climate conditions. *Plant Pathology*, *67*(6), 1307–1320. https://doi.org/10.1111/PPA.12840

Doehlemann, G., Ökmen, B., Zhu, W., & Sharon, A. (2017). Plant Pathogenic Fungi. *Microbiology Spectrum*, *5*(1). https://doi.org/10.1128/MICROBIOLSPEC.FUNK-0023-2016

Doehlemann, G., Wahl, R., Horst, R. J., Voll, L. M., Usadel, B., Poree, F., Stitt, M., Pons-Kühnemann, J., Sonnewald, U., Kahmann, R., & Kämper, J. (2008). Reprogramming a maize plant: transcriptional and metabolic changes induced by the fungal biotroph *Ustilago maydis*. *The Plant Journal*, *56*(2), 181–195. https://doi.org/10.1111/j.1365-313X.2008.03590.x

Donaldson, M. E., Ostrowski, L. A., Goulet, K. M., & Saville, B. J. (2017). Transcriptome analysis of smut fungi reveals widespread intergenic transcription and conserved antisense transcript expression. *BMC Genomics*, *18*(1). https://doi.org/10.1186/s12864-017-3720-8

Donaldson, M. E., & Saville, B. J. (2012). Natural antisense transcripts in fungi. *Molecular Microbiology*, *85*(3), 405–417. https://doi.org/10.1111/j.1365-2958.2012.08125.x

Donaldson, M. E., & Saville, B. J. (2013). Ustilago maydis natural antisense transcript expression alters mRNA stability and pathogenesis. *Molecular Microbiology*, *89*(1), 29–51. https://doi.org/10.1111/mmi.12254

Donoso, A., & Valenzuela, S. (2018). In-field molecular diagnosis of plant pathogens: recent trends and future perspectives. *Plant Pathology*, *67*(7), 1451–1461. https://doi.org/10.1111/PPA.12859

Enjalbert, B., Smith, D. A., Cornell, M. J., Alam, I., Nicholls, S., Brown, A. J. P., &

Quinn, J. (2006). Role of the Hog1 Stress-activated Protein Kinase in the Global Transcriptional Response to Stress in the Fungal Pathogen Candida albicans □ D. *Molecular Biology of the Cell*, *17*, 1018–1032. https://doi.org/10.1091/mbc.E05-06

FAO. (2021). *World food and agriculture - statistical yearbook 2021*. https://www.fao.org/3/cb4477en/cb4477en.pdf

FAU1 | SGD. (n.d.). Retrieved October 25, 2022, from https://www.yeastgenome.org/locus/S000000985

Fausto, A., Rodrigues, M. L., & Coelho, C. (2019). The still underestimated problem of fungal diseases worldwide. In *Frontiers in Microbiology* (Vol. 10, Issue FEB). Frontiers Media S.A. https://doi.org/10.3389/fmicb.2019.00214

Fisher, M. C., Gurr, S. J., Cuomo, C. A., Blehert, D. S., Jin, H., Stukenbrock, E. H., Stajich, J. E., Kahmann, R., Boone, C., Denning, D. W., Gow, N. A. R., Klein, B. S., Kronstad, J. W., Sheppard, D. C., Taylor, J. W., Wright, G. D., Heitman, J., Casadevall, A., & Cowen, L. E. (2020). Threats posed by the fungal kingdom to humans, wildlife, and agriculture. *MBio*, *11*(3). https://doi.org/10.1128/MBIO.00449-20/ASSET/6C4AE09A-A3CA-418B-BFCD-09EB1B657093/ASSETS/GRAPHIC/MBIO.00449-20-F0001.JPEG

Flor-Parra, I., Castillo-Lluva, S., & Pérez-Martín, J. (2007). Polar growth in the infectious hyphae of the phytopathogen Ustilago maydis depends on a virulence-specific cyclin. *Plant Cell*, *19*(10), 3280–3296. https://doi.org/10.1105/tpc.107.052738

Fones, H. N., Bebber, D. P., Chaloner, T. M., Kay, W. T., Steinberg, G., & Gurr, S. J. (2020). Threats to global food security from emerging fungal and oomycete crop pathogens. *Nature Food 2020 1:6*, *1*(6), 332–342. https://doi.org/10.1038/s43016-020-0075-0

Gasch, A. P., Spellman, P. T., Kao, C. M., Carmel-Harel, O., Eisen, M. B., Storz, G., Botstein, D., & Brown, P. O. (2000). Genomic expression programs in the response of yeast cells to environmental changes. *Molecular Biology of the Cell*, *11*(12), 4241–4257. https://doi.org/10.1091/mbc.11.12.4241

Gebrie, S. A. (2016). *Biotrophic Fungi Infection and Plant Defense Mechanism*. https://doi.org/10.4172/2157-7471.1000378

Goulet, K. M., Storfie, E. R. M., & Saville, B. J. (2020). Exploring links between antisense RNAs and pathogenesis in Ustilago maydis through transcript and gene characterization. *Fungal Genetics and Biology*, *134*, 103283. https://doi.org/10.1016/J.FGB.2019.103283

Harrison, B., Yazgan, O., Krebs, J. E., & Harrison, B. R. (2009). Life without RNAi: noncoding RNAs and their functions in Saccharomyces cerevisiae. *Article in Biochemistry and Cell Biology*, *87*(5), 767–779. https://doi.org/10.1139/O09-043

Hatmi, S., Villaume, S., Trotel-Aziz, P., Barka, E. A., Clément, C., & Aziz, A. (2018). Osmotic Stress and ABA Affect Immune Response and Susceptibility of Grapevine Berries to Gray Mold by Priming Polyamine Accumulation. *Frontiers in Plant Science*, *9*. https://doi.org/10.3389/FPLS.2018.01010

Hawksworth, D. L., & Lücking, R. (2017). Fungal Diversity Revisited: 2.2 to 3.8 Million Species. *Microbiology Spectrum*, *5*(4). https://doi.org/10.1128/microbiolspec.funk-0052-2016

Ho, E. C. H., Cahill, M. J., & Saville, B. J. (2007). Gene discovery and transcript analyses in the corn smut pathogen Ustilago maydis: Expressed sequence tag and genome sequence comparison. *BMC Genomics*, *8*. https://doi.org/10.1186/1471-2164-8-334

HTA2 | SGD. (n.d.). Retrieved October 25, 2022, from https://www.yeastgenome.org/locus/S000000099

Hussain, S., Ulhassan, Z., Brestic, M., Zivcak, M., Weijun Zhou, Allakhverdiev, S. I., Yang, X., Safdar, M. E., Yang, W., & Liu, W. (2021). Photosynthesis research under climate change. *Photosynthesis Research*, *150*(1–3), 5–19. https://doi.org/10.1007/S11120-021-00861-Z/TABLES/1

Jeon, J., Kwon, S., & Lee, Y. H. (2014). Histone Acetylation in Fungal Pathogens of Plants. *The Plant Pathology Journal*, *30*(1), 1. https://doi.org/10.5423/PPJ.RW.01.2014.0003

José De Assis, L., Manfiolli, A., Mattos, E., Fabri, J. H. T. M., Malavazi, I., Jacobsen, I. D., Brock, M., Cramer, R. A., Thammahong, A., Hagiwara, D., Nicolas, L., Ries, A., Goldman, G. H., & Yu, H. (2018). *Protein Kinase A and High-Osmolarity Glycerol Response Pathways Cooperatively Control Cell Wall Carbohydrate Mobilization in Aspergillus fumigatus*. https://doi.org/10.1128/mBio

Kämper, J., Kahmann, R., Bölker, M., Ma, L. J., Brefort, T., Saville, B. J., Banuett, F., Kronstad, J. W., Gold, S. E., Müller, O., Perlin, M. H., Wösten, H. A. B., De Vries, R., Ruiz-Herrera, J., Reynaga-Peña, C. G., Snetselaar, K., McCann, M., Pérez-Martín, J., Feldbrügge, M., … Birren, B. W. (2006). Insights from the genome of the biotrophic fungal plant pathogen Ustilago maydis. *Nature 2006 444:7115*, *444*(7115), 97–101. https://doi.org/10.1038/nature05248

Koeck, M., Hardham, A. R., & Dodds, P. N. (2011). The role of effectors of biotrophic and hemibiotrophic fungi in infection. *Cellular Microbiology*, *13*(12), 1849. https://doi.org/10.1111/J.1462-5822.2011.01665.X

Lanver, D., Berndt, P., Tollot, M., Naik, V., Vranes, M., Warmann, T., Münch, K., Rössel, N., & Kahmann, R. (2014). Plant Surface Cues Prime Ustilago maydis for Biotrophic Development. *PLoS Pathogens*, *10*(7). https://doi.org/10.1371/journal.ppat.1004272

Lanver, D., Müller, A. N., Happel, P., Schweizer, G., Haas, F. B., Franitza, M., Pellegrin, C., Reissmann, S., Altmüller, J., Rensing, S. A., & Kahmann, R. (2018). The Biotrophic Development of Ustilago maydis Studied by RNA-Seq Analysis. *The Plant Cell*, *30*(2), 300–323. https://doi.org/10.1105/TPC.17.00764

Lapidot, M., & Pilpel, Y. (2006). Genome-wide natural antisense transcription: coupling its regulation to its different regulatory mechanisms. *EMBO Reports*, *7*(12), 1216–1222. https://doi.org/10.1038/SJ.EMBOR.7400857

Laurie, J. D., Ali, S., Linning, R., Mannhaupt, G., Wong, P., Güldener, U., Münsterkötter, M., Moore, R., Kahmann, R., Bakkeren, G., & Schirawski, J. (2012). Genome Comparison of Barley and Maize Smut Fungi Reveals Targeted Loss of RNA Silencing Components and Species-Specific Presence of Transposable Elements. *The Plant Cell*, *24*(5), 1733–1745. https://doi.org/10.1105/TPC.112.097261

Laurie, J. D., Linning, R., & Bakkeren, G. (2008). Hallmarks of RNA silencing are found in the smut fungus Ustilago hordei but not in its close relative Ustilago maydis. *Current Genetics*, *53*(1), 49–58. https://doi.org/10.1007/S00294-007-0165-7/FIGURES/4

Leong, H. S., Dawson, K., Wirth, C., Li, Y., Connolly, Y., Smith, D. L., Wilkinson, C. R. M., & Miller, C. J. (2014). A global non-coding RNA system modulates fission yeast protein levels in response to stress. *Nature Communications 2014 5:1*, *5*(1), 1–10. https://doi.org/10.1038/ncomms4947

Li, J., Liu, X., Yin, Z., Hu, Z., & Zhang, K. Q. (2021). An Overview on Identification and Regulatory Mechanisms of Long Non-coding RNAs in Fungi. *Frontiers in Microbiology*, *12*, 995. https://doi.org/10.3389/FMICB.2021.638617/BIBTEX

Liebal, U. W., Ullmann, L., Lieven, C., Kohl, P., Wibberg, D., Zambanini, T., & Blank, L. M. (2022). *A Genome-Scale Metabolic Model for the Smut-Fungus Usti-lago maydis*. https://doi.org/10.1101/2022.03.03.482780

Liu, B., Xiang, W., Liu, J., Tang, J., Wang, J., Liu, B., Long, Z., Wang, L., Yin, G., & Liu, J. (2021). The regulatory role of antisense lncRNAs in cancer. *Cancer Cell International 2021 21:1*, *21*(1), 1–15. https://doi.org/10.1186/S12935-021-02168-4

Lorrain, C., Gonçalves dos Santos, K. C., Germain, H., Hecker, A., & Duplessis, S. (2019). Advances in understanding obligate biotrophy in rust fungi. *New Phytologist*, *222*(3), 1190–1206. https://doi.org/10.1111/NPH.15641

Lucca, A. J. De. (2007). Harmful fungi in both agriculture and medicine. *Rev Iberoam Micol*, *24*(1), 3–13.

Magan, N., Medina, A., & Aldred, D. (2011). Possible climate-change effects on mycotoxin contamination of food crops pre- and postharvest. *Plant Pathology*, *60*(1), 150–163. https://doi.org/10.1111/J.1365-3059.2010.02412.X

Maja, M. M., & Ayano, S. F. (2021). The Impact of Population Growth on Natural Resources and Farmers' Capacity to Adapt to Climate Change in Low-Income Countries. *Earth Systems and Environment*, *5*(2), 271–283. https://doi.org/10.1007/S41748-021-00209-6/FIGURES/5

Mäkelä, M. R., Donofrio, N., & De Vries, R. P. (2014). Plant biomass degradation by fungi. *Fungal Genetics and Biology*, *72*, 2–9. https://doi.org/10.1016/J.FGB.2014.08.010

Mapuranga, J., Zhang, N., Zhang, L., Chang, J., & Yang, W. (2022). Infection Strategies and Pathogenicity of Biotrophic Plant Fungal Pathogens. *Frontiers in Microbiology*, *13*. https://doi.org/10.3389/FMICB.2022.799396

Molina, L., & Kahmann, R. (2007). An Ustilago maydis Gene Involved in H2O2 Detoxification Is Required for Virulence. *The Plant Cell*, *19*(7), 2293–2309. https://doi.org/10.1105/TPC.107.052332

Möller, M., & Stukenbrock, E. H. (2017). Evolution and genome architecture in fungal plant pathogens. *Nature Reviews Microbiology*, *15*(12), 756–772. https://doi.org/10.1038/NRMICRO.2017.76

Molotoks, A., Smith, P., & Dawson, T. P. (2021). Impacts of land use, population, and climate change on global food security. *Food and Energy Security*, *10*(1), e261. https://doi.org/10.1002/FES3.261

Morrison, E. N., Donaldson, M. E., & Saville, B. J. (2012). Identification and analysis of genes expressed in the Ustilago maydis dikaryon: uncovering a novel class of pathogenesis genes. *Canadian Journal of Plant Pathology*, *34*(3), 417–435. https://doi.org/10.1080/07060661.2012.697077

Naranjo-Ortiz, M. A., & Gabaldón, T. (2019). Fungal evolution: major ecological adaptations and evolutionary transitions. *Biological Reviews*, *94*(4), 1443–1476. https://doi.org/10.1111/BRV.12510

Newton, A. C., Johnson, S. N., & Gregory, P. J. (2011). Implications of climate change for diseases, crop yields and food security. In *Euphytica* (Vol. 179, Issue 1, pp. 3–18). https://doi.org/10.1007/s10681-011-0359-4

Nikolaou, E., Agrafioti, I., Stumpf, M., Quinn, J., Stansfield, I., & Brown, A. J. (2009).

Phylogenetic diversity of stress signalling pathways in fungi. *BMC Evolutionary Biology*, *9*(1), 44. https://doi.org/10.1186/1471-2148-9-44

Nnadi, N. E., & Carter, D. A. (2021). Climate change and the emergence of fungal pathogens. *PLOS Pathogens*, *17*(4), e1009503. https://doi.org/10.1371/JOURNAL.PPAT.1009503

Olicón-Hernández, D. R., Araiza-Villanueva, M. G., Pardo, J. P., Aranda, E., & Guerra-Sánchez, G. (2019). New Insights of Ustilago maydis as Yeast Model for Genetic and Biotechnological Research: A Review. *Current Microbiology 2019 76:8*, *76*(8), 917–926. https://doi.org/10.1007/S00284-019-01629-4

Oshiro, J., Han, G. S., Iwanyshyn, W. M., Conover, K., & Carman, G. M. (2003). Regulation of the yeast DPP1-encoded diacylglycerol pyrophosphate phosphatase by transcription factor Gis1p. *Journal of Biological Chemistry*, *278*(34), 31495–31503. https://doi.org/10.1074/jbc.M305452200

Ostrowski, L. A., & Saville, B. J. (2017). Natural antisense transcripts are linked to the modulation of mitochondrial function and teliospore dormancy in *Ustilago maydis*. *Molecular Microbiology*, *103*(5), 745–763. https://doi.org/10.1111/mmi.13587

Owttrim, G. W. (2006). RNA helicases and abiotic stress. *Nucleic Acids Research*, *34*(11), 3220. https://doi.org/10.1093/NAR/GKL408

Peay, K. G., Kennedy, P. G., & Talbot, J. M. (2016). *Dimensions of biodiversity in the Earth mycobiome*. https://doi.org/10.1038/nrmicro.2016.59

Pelechano, V., & Steinmetz, L. M. (2013). Gene regulation by antisense transcription. *Nature Reviews Genetics*, *14*(12), 880–894. https://doi.org/10.1038/NRG3594

PHO80 | SGD. (n.d.). Retrieved March 25, 2020, from https://www.yeastgenome.org/locus/S000005361

Pradhan, A., Ma, Q., De Assis, L. J., Leaves, I., Larcombe, D. E., Rodriguez Rondon, A. V, Nev, O. A., & Brown, A. J. P. (2021). Anticipatory Stress Responses and Immune Evasion in Fungal Pathogens. *Trends in Microbiology*, *29*, 416–427. https://doi.org/10.1016/j.tim.2020.09.010

Rausher, M. D. (2001). Co-evolution and plant resistance to natural enemies. *Nature 2001 411:6839*, *411*(6839), 857–864. https://doi.org/10.1038/35081193

Redkar, A., Matei, A., & Doehlemann, G. (2017). Insights into host cell modulation and induction of new cells by the corn smut Ustilago maydis. *Frontiers in Plant Science*, *8*. https://doi.org/10.3389/fpls.2017.00899

Ristaino, J. B., Anderson, P. K., Bebber, D. P., Brauman, K. A., Cunniffe, N. J., Fedoroff, N. V., Finegold, C., Garrett, K. A., Gilligan, C. A., Jones, C. M., Martin, M. D., MacDonald, G. K., Neenan, P., Records, A., Schmale, D. G., Tateosian, L., & Wei, Q. (2021). The persistent threat of emerging plant disease pandemics to global food security. *Proceedings of the National Academy of Sciences of the United States of America*, *118*(23). https://doi.org/10.1073/PNAS.2022239118/SUPPL_FILE/PNAS.2022239118.SAPP.PDF

Rutherford, J. C., Bahn, Y. S., Van Den Berg, B., Heitman, J., & Xue, C. (2019). Nutrient and stress sensing in pathogenic yeasts. In *Frontiers in Microbiology* (Vol. 10, Issue MAR, p. 442). Frontiers Media S.A. https://doi.org/10.3389/fmicb.2019.00442

Salmerón-Santiago, K. G., Pardo, J. P., Flores-Herrera, O., Mendoza-Hernández, G., Miranda-Arango, M., & Guerra-Sánchez, G. (2011). Response to osmotic stress and temperature of the fungus Ustilago maydis. In *Archives of Microbiology* (Vol. 193,

Issue 10, pp. 701–709). Springer. https://doi.org/10.1007/s00203-011-0706-9
Santini, A., & Ghelardini, L. (2015). Plant pathogen evolution and climate change. *CAB Reviews Perspectives in Agriculture Veterinary Science Nutrition and Natural Resources*, *10*(35). https://doi.org/10.1079/PAVSNNR201510035
Savary, S., Willocquet, L., Pethybridge, S. J., Esker, P., McRoberts, N., & Nelson, A. (2019). The global burden of pathogens and pests on major food crops. *Nature Ecology & Evolution 2019 3:3*, *3*(3), 430–439. https://doi.org/10.1038/s41559-018-0793-y
Saville, B. J., Donaldson, M. E., & Doyle, C. E. (2012). Investigating Host Induced Meiosis in a Fungal Plant Pathogen. *Meiosis - Molecular Mechanisms and Cytogenetic Diversity*. https://doi.org/10.5772/30032
Scholthof, K. B. G. (2007). The disease triangle: pathogens, the environment and society. *Nature Reviews Microbiology*, *5*(2), 152–156. https://doi.org/10.1038/nrmicro1596
Schwartz, S., Bernstein, D. A., Mumbach, M. R., Jovanovic, M., Herbst, R. H., León-Ricardo, B. X., Engreitz, J. M., Guttman, M., Satija, R., Lander, E. S., Fink, G., & Regev, A. (2014). Transcriptome-wide mapping reveals widespread dynamic regulated pseudouridylation of ncRNA and mRNA. *Cell*, *159*(1), 148. https://doi.org/10.1016/J.CELL.2014.08.028
Shi, X., Zou, Y., Chen, Y., Zheng, C., & Ying, H. (2016). Overexpression of a water-forming NADH oxidase improves the metabolism and stress tolerance of saccharomyces cerevisiae in aerobic fermentation. *Frontiers in Microbiology*, *7*(SEP). https://doi.org/10.3389/fmicb.2016.01427
Singh, S., Sahu, R. K., Sugathan, A., & Tomar, R. S. (2021). The H2A N-terminal tail is required to alleviate copper-induced stress in Saccharomyces cerevisiae. *FEMS Yeast Research*, *21*(8), 61. https://doi.org/10.1093/FEMSYR/FOAB061
Soontorngun, N., Baramee, S., Tangsombatvichit, C., Thepnok, P., Cheevadhanarak, S., Robert, F., & Turcotte, B. (2012). Genome-wide location analysis reveals an important overlap between the targets of the yeast transcriptional regulators Rds2 and Adr1. *Biochemical and Biophysical Research Communications*, *423*(4), 632–637. https://doi.org/10.1016/J.BBRC.2012.05.151
Strunk, B. S., & Karbstein, K. (2009). Powering through ribosome assembly. In *RNA* (Vol. 15, Issue 12, pp. 2083–2104). Cold Spring Harbor Laboratory Press. https://doi.org/10.1261/rna.1792109
Tian, X., Engel, B. A., Qian, H., Hua, E., Sun, S., & Wang, Y. (2021). Will reaching the maximum achievable yield potential meet future global food demand? *Journal of Cleaner Production*, *294*, 126285. https://doi.org/10.1016/J.JCLEPRO.2021.126285
Tisseur, M., Kwapisz, M., & Morillon, A. (2011). Pervasive transcription - Lessons from yeast. In *Biochimie* (Vol. 93, Issue 11, pp. 1889–1896). Elsevier. https://doi.org/10.1016/j.biochi.2011.07.001
Toke, D. A., Bennett, W. L., Dillon, D. A., Wu, W. I., Chen, X., Ostrander, D. B., Oshiro, J., Cremesti, A., Voelker, D. R., Fischl, A. S., & Carman, G. M. (1998). Isolation and characterization of the Saccharomyces cerevisiae DPP1 gene encoding diacylglycerol pyrophosphate phosphatase. *Journal of Biological Chemistry*, *273*(6), 3278–3284. https://doi.org/10.1074/jbc.273.6.3278
TOP2 | SGD. (n.d.). Retrieved October 25, 2022, from https://www.yeastgenome.org/locus/S000005032
Torres, D. E., Oggenfuss, U., Croll, D., & Seidl, M. F. (2020). Genome evolution in

fungal plant pathogens: looking beyond the two-speed genome model. *Fungal Biology Reviews*, *34*(3), 136–143. https://doi.org/10.1016/J.FBR.2020.07.001
United Nations. (2018). *The Sustainable Development Goals Report 2018*. https://unstats.un.org/sdgs/files/report/2018/TheSustainableDevelopmentGoalsReport2018-EN.pdf
United Nations. (2022a). *The Sustainable Development Goals Report 2022*.
United Nations. (2022b). *World Population Prospects 2022 Summary of Results*.
Velásquez, A. C., Castroverde, C. D. M., & He, S. Y. (2018). Plant–Pathogen Warfare under Changing Climate Conditions. In *Current Biology* (Vol. 28, Issue 10, pp. R619–R634). Cell Press. https://doi.org/10.1016/j.cub.2018.03.054
Vu, B. G., & Moye-Rowley, W. S. (2018). Construction and use of a recyclable marker to examine the role of major facilitator superfamily protein members in Candida glabrata drug resistance phenotypes. *MSphere*, *3*(2). https://doi.org/10.1128/msphere.00099-18
Wakelin, S. A., Gomez-Gallego, M., Jones, E., Smaill, S., Lear, G., & Lambie, S. (2018). Climate change induced drought impacts on plant diseases in New Zealand. *Australasian Plant Pathology 2018 47:1*, *47*(1), 101–114. https://doi.org/10.1007/S13313-018-0541-4
Wang, J., Meng, X., Dobrovolskaya, O. B., Orlov, Y. L., & Chen, M. (2017). Non-coding RNAs and Their Roles in Stress Response in Plants. *Genomics, Proteomics & Bioinformatics*, *15*(5), 301–312. https://doi.org/10.1016/J.GPB.2017.01.007
Werner-Washburne, M., Braun, E., Johnston, G. C., & Singer, R. A. (1993). Stationary phase in the yeast Saccharomyces cerevisiae. *Microbiological Reviews*, *57*(2), 383–401. https://doi.org/10.1128/MR.57.2.383-401.1993
Wight, M., & Werner, A. (2013). The functions of natural antisense transcripts. *Essays in Biochemistry*, *54*(1), 91. https://doi.org/10.1042/BSE0540091
Wing, I. S., De Cian, E., & Mistry, M. N. (2021). Global vulnerability of crop yields to climate change. *Journal of Environmental Economics and Management*, *109*, 102462. https://doi.org/10.1016/J.JEEM.2021.102462
Yang, J., Chen, D., Matar, K. A. O., Zheng, T., Zhao, Q., Xie, Y., Gao, X., Li, M., Wang, B., & Lu, G. dong. (2020). The deubiquitinating enzyme MoUbp8 is required for infection-related development, pathogenicity, and carbon catabolite repression in Magnaporthe oryzae. *Applied Microbiology and Biotechnology*, *104*(11), 5081–5094. https://doi.org/10.1007/S00253-020-10572-5
Zhang, X. M., Chang, Q., Zeng, L., Gu, J., Brown, S., & Basch, R. S. (2006). TBLR1 regulates the expression of nuclear hormone receptor co-repressors. *BMC Cell Biology*, *7*, 31. https://doi.org/10.1186/1471-2121-7-31
Zulfiqar, F., Akram, N. A., & Ashraf, M. (2019). Osmoprotection in plants under abiotic stresses: new insights into a classical phenomenon. *Planta 2019 251:1*, *251*(1), 1–17. https://doi.org/10.1007/S00425-019-03293-1
Zulfiqar, F., & Ashraf, M. (2021). Bioregulators: unlocking their potential role in regulation of the plant oxidative defense system. *Plant Molecular Biology*, *105*(1–2), 11–41. https://doi.org/10.1007/S11103-020-01077-W/FIGURES/4